J|A|C|S
ARTICLES
Published on Web 06/11/2005

Docking, Triggering, and Biological Activity of Dynemicin A in DNA: A Computational Study

Tell Tuttle,† Elfi Kraka,* and Dieter Cremer
Contribution from the Department of Chemistry and Department of Physics, University of the Pacific, 3601 Pacific Avenue, Stockton, California 95211-0110

Received June 24, 2004; E-mail: ekraka@pacific.edu; dcramer@pacific.edu

Abstract: The triggering and biological activity of the naturally occurring enediyne dynemicin A (**1**) was investigated, both inside and outside the minor groove of the duplex 10-mer B-DNA sequence d(CTACTACTGG)·d(CCAGTAGTAG), using density functional theory (B3LYP with the 3-21G and 6-31G-(d) basis set), BD(T)/cc-pVDZ (Brueckner doubles with a perturbative treatment of triple excitations), and the ONIOM approach. Enediyne **1** is triggered by NADPH in a strongly exothermic reaction (−88 kcal/mol), which involves a number of intermediate steps. Untriggered **1** has a high barrier for the Bergman cyclization (52 kcal/mol) that is lowered after triggering to 16.7 kcal/mol due to an epoxide opening and the accompanying strain relief. The Bergman reaction of triggered **1** is slightly exothermic by 2.8 kcal/mol. The singlet biradical formed in this reaction is kinetically stable (activation enthalpies of 19.5 and 21.8 kcal/mol for retro-Bergman reactions) and is as reactive as *para*-benzyne. The activity-relevant docking mode is an edge-on insertion into the minor groove, whereas the intercalation between base pairs, although leading to larger binding energies, excludes a triggering of **1** and the development of its biological activity. Therefore, an insertion−intercalation model is developed, which can explain all known experimental observations made for **1**. On the basis of the insertion−intercalation model it is explained why large intercalation energies suppress the biological activity of dynemicin and why double-strand scission can be achieved only in a two-step mechanism that involves two enediyne molecules, explaining thus the high ratio of single-strand to double-strand scission observed for **1**.

I. Introduction

Dynemicin A (**1**), a member of the enediyne family of antibiotics, was discovered in 1989 when it was isolated from a fermentation broth of *Micromonospora chersina* as a violet-colored solid.[1] The structure of **1** was expeditiously determined from the X-ray diffraction studies of the closely related compound triacetyldynemicin A.[2] This structure was later confirmed by the total synthesis of **1**[3] and the determination of the X-ray diffraction geometry of deoxy-dynemicin A.[4] Enediyne **1** is composed of a ring system (rings A, B, C, D, E, F, see Scheme 1) including an anthraquinone moiety (A, B, C: *the triggering device*[5]) and a 10-membered enediyne unit (F: *the warhead*[5]), which bridges the two six-membered rings D and E. The presence of the anthraquinone moiety in the molecule is in contrast to the other members of the family such as calicheamicin γ^1 and esperamicin A, which have oligosaccharide tails.[5] This difference makes **1** a particularly appealing candidate for quantum chemical studies because its structure is both relatively rigid and compact.

Scheme 1. Atom Numbering and Ring Notation of Dynemicin **1**

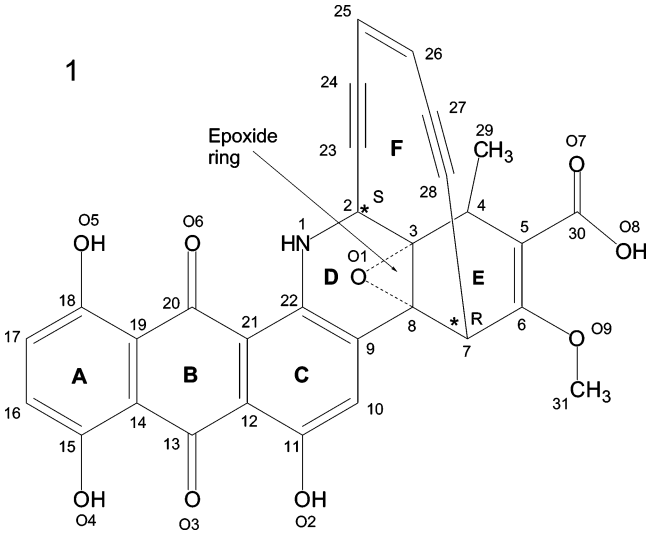

The structural differences between **1** and the other members of the enediyne family of antibiotics suggest that a different mechanism of binding to DNA may be employed, as both

† Present address: Max-Planck-Institut für Kohlenforschung, Kaiser-Wilhelm-Platz 1, D-45470, Mülheim an der Ruhr, Germany. E-mail: tell@mpimuelheim.mpg.de.

(2) Konishi, M.; Ohkuma, H.; Matsumoto, M.; Tsuno, T.; Kamei, H.; Miyaki, T.; Oki, T.; Kawaguchi, H.; VanDuyne, G. D.; Clardy, J. *J. Antibiot* **1989**, *42*, 1449.
(3) Konishi, M.; Ohkuma, H.; Tsuno, T.; Oki, T.; VanDuyne, G. D.; Clardy, J. *J. Am. Chem. Soc.* **1990**, *112*, 3715.
(4) (a) Myers, A. G.; Tom, N. J.; Fraley, M. E.; Cohen, S. B.; Madar, D. J. *Chem. Biol.* **1995**, *2*, 33. (b) Myers, A. G.; Tom, N. J.; Fraley, M. E.; Cohen, S. B.; Madar, D. J. *J. Am. Chem. Soc.* **1997**, *119*, 6072.
(5) Shiomi, K.; Iinuma, H.; Naganawa, H.; Hamada, M.; Hattori, S.; Nakamura, H.; Takeuchi, T.; Iitaka, Y. *J. Antibiot.* **1990**, *43*, 1000.
(6) (a) *Enediyne Antibiotics as Antitumor Agents*; Borders, D. B., Doyle, T. W., Eds.; Marcel Dekker: New York, 1995. (b) Konishi M.; Toshikazu O.; In *Enediyne Antibiotics as Antitumor Agents*; Borders, D. B., Doyle, T. W., Eds.; Marcel Dekker: New York, 1995; Chapter 15.

calicheamicin γ^1 and esperamicin A are known to bind to the minor groove through interactions with their oligosaccharide tails. An alternative to the minor groove binding, which could be possible in the case of dynemicin A, is that the anthraquinone unit intercalates between two base pairs of DNA.[6] Several previous molecular dynamics (MD) studies[7−9] have focused on this mode of docking, as it has been able to explain a number of the observed binding properties of the molecule. Such properties include a reduced sequence specificity,[6,7] relative to other minor groove binders,[5] and the preference of **1** for attacking more flexible regions of the DNA, where the physical constraints of the minor groove are more forgiving.[8−13]

Nonetheless, the form of **1** during its proposed intercalation into DNA has been a topic of much debate. Molecular mechanics (MM) and MD studies on the intercalation of dynemicin previously suggested opposing explanations of the process. Either the opening of the epoxide ring (the triggering mechanism) takes place before the molecule is docked,[7,9] or the triggering could occur in the complexed form.[8] In 1995, an experimental investigation by Myers and co-workers supported the proposition of the uncomplexed triggering mechanism.[14] The Myers study showed that when **1** was modified to increase its binding affinity to the DNA, its ability to cleave DNA was decreased. Conversely, those analogues with a lowered binding affinity experienced an increase in activity relative to the number of bound molecules. However, this observation is far from conclusive, as the chemical reality of the highly reactive triggered molecule docking into the DNA, rather than abstracting H atoms from another source, seems unrealistic. Despite this, in all investigations, either experimentally or theoretically, the docking mode of **1** was assumed to correspond to an intercalation between two base pairs.[6−16] In this current study, we will propose a new mechanism for the binding of dynemicin A to DNA, which is congruent with all of the experimental observations and reconciles the question of the timing of the triggering process.

The orientation of the docked molecule is important, not only for the triggering mechanism but because it also addresses the question of the possible H abstraction sites from the DNA. It has been proposed that **1** abstracts H atoms from the DNA in a nonconcomitant manner, i.e., a two-step double-stranded scission (DSS), due to the greater ratio of single-strand to DSSs with dynemicin A, compared to other members of the enediyne family.[9b,10] However, as the positioning of the biradical intermediate involved in the abstraction process in the DNA has not yet been experimentally determined, the reason behind this increased ratio remains unclear.

Enediyne **1** has been shown to have excellent cytotoxicity in the ng/mL range against a number of murine and human tumor cells, when tested in vitro. In addition, it has proven to be extremely potent in vivo when tested on mouse tumor models.[5] In addition to the antitumor activity, dynemicin A was shown to possess a range of antimicrobial activity, on the order of pg/mL against Gram-positive bacteria, ng/mL against Gram-negative bacteria, and μg/mL against fungi.[5] Despite this remarkable activity, it still remains one of the least reactive of the enediyne-containing class of antibiotics. This was originally attributed to the weaker binding abilities of the molecule, compared with other members of the family, e.g., calicheamicin γ^1.[5] However, many other factors may contribute to the reduced activity. The activity of **1** results from a *para*-didehydrobenzene (*para*-benzyne) radical, which is formed via a Bergman cyclization[17] of the enediyne warhead (either **1** → **2** or **6** → **7**, Scheme 2). The biradical is able to abstract H atoms from the DNA, causing strand scission. Thus, both the activation energy of this cyclization[18−22] and the alignment of the radical carbon atoms with the abstraction sites in the complex strongly determine the biological activity.

In this work, we will first consider the question of triggering and its energetic implications, and then we will focus on the preferred docking mode of **1**: Is it possible for **1** to be triggered in its complexed form, and if so, how does this triggering occur? What will be the preferred docking mode: minor groove intercalation, as generally assumed, or minor groove insertion? This will lead to the question of the energetics of the Bergman cyclization in the complexed form where two major aspects have to be considered: (a) Is the cyclization reaction energetically favorable? (b) Is the biradical kinetically stable, such that it can undergo the H abstraction reaction, or does it immediately rearrange via a retro-Bergman reaction to its original form (**1** or **6**) or to an acyclic enediyne (**8** or **9**, Scheme 2)? We will also consider whether the Bergman cyclization of triggered and docked **1** can cause H abstraction in the intercalation (insertion) mode and by this a cleavage of the DNA strand(s). In short, this work reports a new mechanism for the total dynemicin−DNA interaction, from the initial approach of **1** and the preferred docking mode through the Bergman reaction and up to the final H abstraction reaction, which is no longer based on the common docking description of **1** in DNA. This new mechanism will have significant consequences for drug design. The investigation will be based on density functional theory (DFT) calculations in connection with both high-level ab initio and MM calculations described in the next section.

2. Computational Methods

At the level of wave function theory (WFT), the description of the Bergman cyclization requires the use of coupled cluster theory to obtain reliable data, as long-range correlation plays an important role.[23] DFT accounts for some of the long-range effects via its local exchange

(7) Sugiura, Y.; Shiraki, T.; Konishi, M.; Oki, T. *Proc. Natl. Acad. Sci. U.S.A.* **1990**, *87*, 3831.
(8) Langley, D. R.; Doyle, T. W.; Beveridge, D. L. *J. Am. Chem. Soc.* **1991**, *113*, 4395.
(9) Wender, P. A.; Kelly, R. C.; Beckham, S.; Miller, B. L. *Proc. Natl. Acad. Sci. U.S.A.* **1991**, *88*, 8835.
(10) (a) Cardozo, M. G.; Hopfinger, A. J. *Biopolymers* **1993**, *33*, 377. (b) Cardozo, M. G.; Hopfinger, A. J. *Mol. Pharm.* **1991**, *40*, 1023.
(11) Kusakabe, T.; Uesugi, M.; Sugiura, Y. *Biochemistry* **1995**, *34*, 9944.
(12) (a) Kusakabe, T.; Maekawa, K.; Ichikawa, A.; Uesugi, M.; Sugiura, Y. *Biochemistry* **1993**, *32*, 11669. (b) Ichikawa, A.; Kuboya, T.; Aoyama, T.; Sugiura, Y. *Biochemistry* **1992**, *31*, 6784.
(13) Guo, Q.; Lu, M.; Shahrestanifar, M.; Sheardy, R. D.; Kallenbach, N. R. *Biochemistry* **1991**, *30*, 11735.
(14) Lu, M.; Guo, Q.; Kallenbach, N. R. *J. Biomol. Struct. Dyn.* **1991**, *9*, 271.
(15) Myers, A. G.; Cohen, S. B.; Tom, N. J.; Madar, D. J.; Fraley, M. E. *J. Am. Chem. Soc.* **1995**, *117*, 7574.
(16) Unno, R.; Michishita, H.; Inagaki, H.; Suzuki, Y.; Baba, Y.; Jomori, T.; Nishikawa, T.; Isobe M. *Bioorg. Med. Chem.* **1997**, *5*, 987.
(17) Basak, A.; Bdour, H. M.; Shain, J. C.; Mandal, S.; Rudra, K. R.; Nag, S. *Bioorg. Med. Chem. Lett.* **2000**, *10*, 1321.
(18) Bergman, R. G. *Acc. Chem. Res.* **1973**, *6*, 25.
(19) Snyder, J. P.; Tipsword, G. E. *J. Am. Chem. Soc.* **1990**, *112*, 4040.
(20) Ahlström, B.; Kraka, E.; Cremer, D. *Chem. Phys. Lett.* **2002**, *361*, 129.
(21) Jones, G. B.; Warner, P. M. *J. Org. Chem.* **2001**, *66*, 8669.
(22) Tuntiwechapikul, W.; David, W. M.; Kumar, D.; Salazar, M.; Kerwin, S. M. *Biochemistry* **2002**, *41*, 5283.
(23) Alabugin, I. V.; Manoharan, M. *J. Phys. Chem. A* **2003**, *107*, 3363.
(24) (a) Kraka, E.; Cremer, D. *J. Am. Chem. Soc.* **1994**, *116*, 4929. (b) Kraka, E.; Cremer, D. *Chem. Phys. Lett.* **1993**, *216*, 333.

Scheme 2. Reaction Possibilities Leading to the Biological Activity of Dynemicin **1**

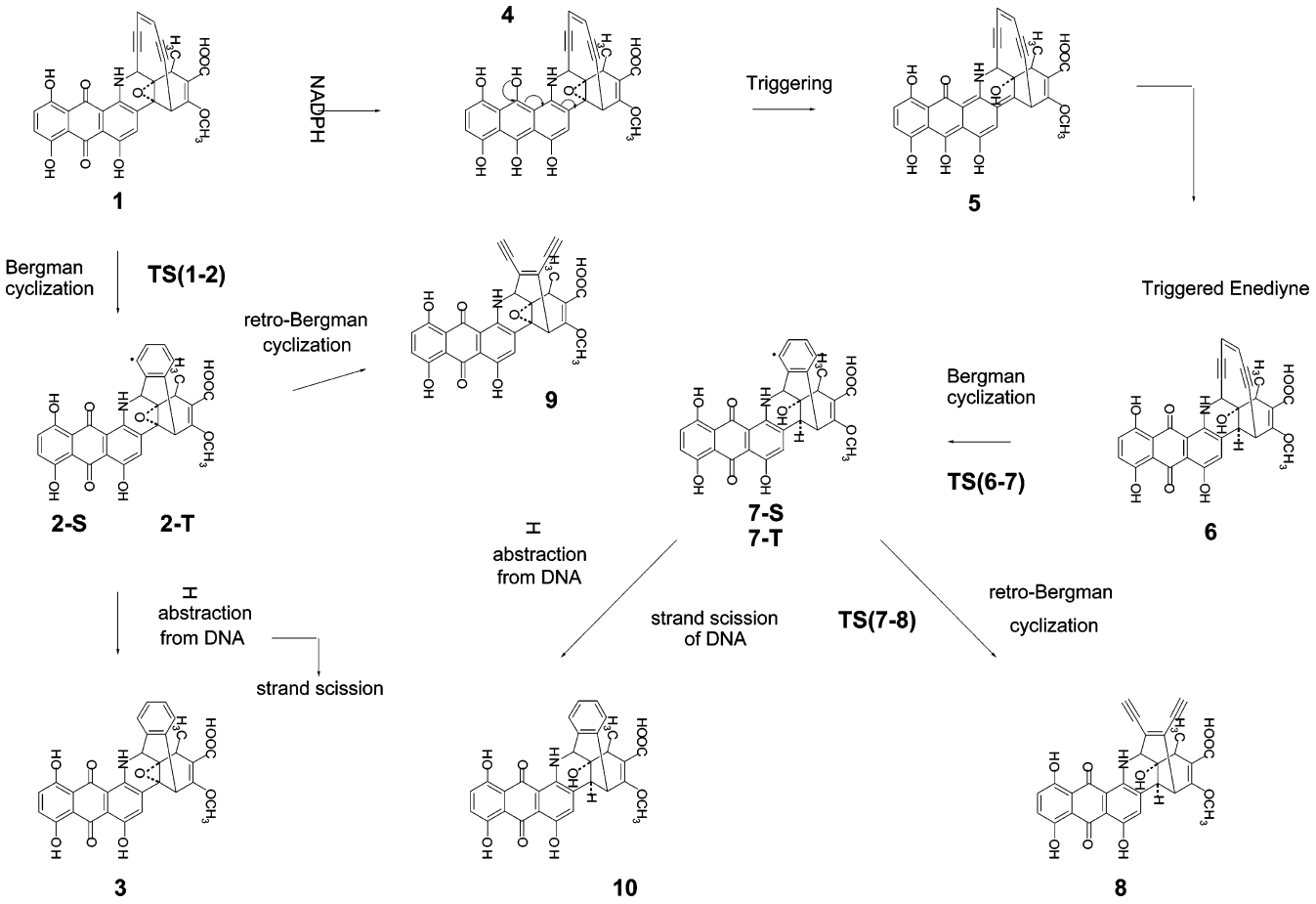

potential and the inherent self-interaction error in an unspecified way.[24,25] Specific long-range correlation can be included into a DFT calculation via a broken-symmetry unrestricted DFT (BS-UDFT) description[26] where the right choice of the exchange−correlation functional is essential to avoid double counting of correlation effects.[27] However, if this is considered, DFT is the method of choice to investigate both model[28−30] and naturally occurring enediynes, as well as their chemical properties.[19]

A DFT description of the Bergman cyclization of **1** requires the calculation of molecules with about 60 atoms, which will imply the use of about 700 basis functions if an augmented valence double-ζ basis set is used. Calculations with such a large number of basis functions are feasible at the DFT level, although for repeated DFT geometry optimizations and frequency calculations of up to 15 structures they still imply a heavy computational load. We note in this connection that the present work is part of a larger project aimed at modifying dynemicin in such a way that it will lead to a new nontoxic antitumor antibiotic. For this purpose, the calculation of more than 50 substituted dynemicin structures was needed, which had to be done consistently at the same level of theory. Previously, we have demonstrated the usefulness of Pople's 3-21G split-valence basis set[31] in connection with the hybrid functional B3LYP[32,33] for describing the Bergman cyclization of **1**.[19] The surprising accuracy of this level of theory results partially because of a fortuitous cancellation of errors, but also from the unique properties of DFT.[34]

Using B3LYP/3-21G, the geometries of the structures shown in Scheme 2, including transition state structures **TS(1−2)**, **TS(6−7)**, and **TS(7−8)**, were fully optimized. This involved energy and gradient calculations with about 400 basis functions for each structure. Restricted DFT (RDFT) calculations were carried out for the closed shell states. However, in each case, the internal and external stability of the RDFT solution was tested.[35] If the latter was not fulfilled, as in the case of the singlet biradicals **2** and **7** (Scheme 2), a BS-UDFT calculation was performed for the singlet state, as BS-UDFT is known to lead to reasonable results for *para*-benzyne biradicals.[26−30,36] The triplet states investigated in this work were calculated at the UDFT level of theory. For the calculations described above, the program packages COLOGNE2004[37] and Gaussian03[38] were used.

(25) (a) Polo, V.; Kraka, E.; Cremer, D. *Mol. Phys.* **2002**, *100*, 1771. (b) Polo, V.; Kraka, E.; Cremer, D. *Theor. Chem. Acc.* **2002**, *107*, 291. (c) Polo, V.; Gräfenstein, J.; Kraka, E.; Cremer, D. *Chem. Phys. Lett.* **2002**, *352*, 469. (d) Polo, V.; Gräfenstein, J.; Kraka, E.; Cremer, D. *Theor. Chem. Acc.* **2003**, *109*, 22.
(26) (a) Gräfenstein, J.; Kraka, E.; Cremer, D. *J. Chem. Phys.* **2004**, *120*, 524. (b) Gräfenstein, J.; Kraka, E.; Cremer, D. *Phys. Chem. Chem. Phys.* **2004**, *6*, 1096.
(27) Gräfenstein, J.; Kraka, E.; Filatov, M.; Cremer, D. *Int. J. Mol. Sci.* **2002**, *3*, 360.
(28) Cremer, D.; Filatov, M.; Polo, V.; Kraka, E.; Shaik, S. *Int. J. Mol. Sci.* **2002**, *3*, 604.
(29) Gräfenstein, J.; Hjerpe, A.; Kraka, E.; Cremer, D. *J. Phys. Chem. A* **2000**, *104*, 1748.
(30) (a) Kraka, E.; Cremer, D. *J. Comput. Chem.* **2000**, *22*, 216. (b) Kraka, E.; Cremer, D. *J. Mol. Struct. THEOCHEM* **2000**, *506*, 191.
(31) Kraka, E.; Cremer, D. *J. Am. Chem. Soc.* **2000**, *122*, 8245.
(32) Binkley, J. S.; Pople, J. A.; Hehre, W. J. *J. Am. Chem. Soc.* **1980**, *102*, 939.
(33) Becke, A. D. *J. Chem. Phys.* **1993**, *98*, 5648.
(34) (a) Becke, A. D. *Phys. Rev. A* **1988**, *38*, 3098. (b) Lee, C.; Yang. W.; Parr. R. G. *Phys. Rev.* **1988**, *B37*, 785.
(35) Cremer, D. *Mol. Phys.* **2001**, *99*, 1899.
(36) (a) Seeger, R.; Pople J. A. *J. Chem. Phys.* **1977**, *66*, 3045. (b) Bauernschmitt, R.; Ahlrichs, R. *J. Chem. Phys.* **1996**, *104*, 9047.
(37) Marquardt, R.; Balster, A.; Sander, W.; Kraka, E.; Cremer, D.; Radziszewski, J. G. *Angew. Chem.* **1998**, *110*, 1001.
(38) Kraka, E.; Gräfenstein, J.; Filatov, M.; He, Y.; Gauss, J.; Wu, A.; Polo, V.; Olsson, L.; Konkoli, Z.; He, Z.; Cremer, D. COLOGNE2004; Göteborg University, Göteborg, 2004.

Convergence of the geometry optimization depends strongly on the quality of the starting geometry. In the case of **1**, the crystal structure[4] was taken as the starting geometry, with a hydroxide group and hydrogens added using Sybyl.[39] There are no reported experimental geometries for subsequent structures along the reaction path, neither after the epoxide ring opening to form the triggered structure **6** nor after the Bergman cyclization that results in the highly labile singlet biradical **7** and the potential product **10** (Scheme 2). Therefore, at each step (k) along the proposed reaction path the optimized geometry was modified to form the ($k + 1$)th reaction species, which was then reoptimized.

Frequency calculations were carried out for the optimized geometries to obtain thermochemical corrections (zero-point energies, thermal corrections) as well as to ensure the attainment of the correct TS by the presence of just a single imaginary frequency, describing bond formation (breakage) in the TS structures investigated. The thermal corrections found were used to obtain activation enthalpies $\Delta H^a(298)$, reaction enthalpies $\Delta H_R(298)$, and singlet−triplet splittings $\Delta H(S - T)$ at 298 K. In addition, entropies $S(298)$ and free energies $\Delta G^a(298)$ or $\Delta G_R(298)$ were calculated. In view of the biological activity of **1**, it is appropriate to discuss all calculated enthalpies (free energies) with regard to body temperature (310 K). Therefore, all thermochemical corrections were calculated for both 298 and 310 K. However, enthalpy differences between these two temperatures are so small that it is sufficient to report only values for 298 K, although the discussion will frequently refer to body temperature.

The B3LYP/3-21G results were checked in two ways: (a) Single-point B3LYP calculations with the 6-31G(d) basis set[40] were carried out to provide a better description of the strained ring system, especially the three-membered oxirane ring, with the help of the d-type polarization functions. (b) The Bergman reaction steps (Scheme 2) were investigated with the help of a two-layer ONIOM (ONIOM2) method.[41] For this purpose the reaction complex was partitioned into a kernel comprising the six enediyne carbon atoms C23 to C28 and the H atoms at C25 and C26 (Scheme 1) and a periphery comprising the rest of **1**. The kernel was described with coupled cluster theory using Brueckner orbitals,[42] Dunning's cc-pVDZ basis set,[40] and all double excitations. Triple excitations were included in perturbative manner, leading to BD(T), which is known to yield very accurate results.[43] The rest of the molecule was described at the B3LYP/3-21G level of theory. The separation between kernel and periphery was accomplished by replacing C2 and C7 by H atoms. The ONIOM2 energy was obtained with the help of eq 1.

$$E(\text{ONIOM2}) = E(\text{BD(T), kernel}) + E(\text{B3LYP, Real}) - E(\text{B3LYP, kernel}) \quad (1)$$

where E(B3LYP, Real) is the energy of the total molecule calculated with the lower level method.

Docking Studies. The energy calculations aided in determining the most likely reaction mechanism, and each structure, located at a stationary point along the reaction path, was docked into the duplex 10-mer B-DNA sequence d(CTACTACTGG)·d(CCAGTAGTAG). This sequence was selected as it has previously been used in DNA cleavage experiments with **1** and the preferential hydrogen abstraction site has also been determined.[6] The duplex was constructed in HyperChem-(TM)[44] and was minimized in vacuo to 0.01 kcal (mol Å)$^{-1}$. The Amber94[45] parameter set was used for the minimization procedure in conjunction with the Ploak−Ribiere conjugate gradient method implemented in HyperChem(TM).

In this work we did not investigate the sequence selectivity of **1**. Instead we started from the experimental fact that **1**, once triggered and rearranged to a biradical, causes the abstraction of hydrogen atom H5′(G7). Therefore we investigated two different classes of minor groove docking modes that could lead to an abstraction of H5′(G7): (a) intercalation between base pairs A9T2 and T8A3, T8A3 and G7C4, A6T5 and T5A6, T5A6 and G4C7; (b) an edge-on insertion into the minor groove. For the intercalation cases, the DNA was reoptimized to form a cavity for the anthraquinone part of **1**. This led to a widening of the opening between the base pairs from 3−4 Å to about 7−8 Å.

The DNA used in the docking studies was minimized using the CHARMM force field for nucleic acids[46] as implemented in the CHARMM program.[47] An initial minimization was done for the uncomplexed DNA segment, resulting in the canonical B-form DNA. This structure was used in the docking studies for the insertion mechanism. In the case of the intercalation mechanism, the DNA segment was reminimized with the ligand fixed in the desired intercalation site. The CHARMM parameters for the ligand were created in an ad hoc manner using the program QUANTA98 from Molecular Simulations, Inc., Waltham, MA. The QUANTA98 parameters[48] are not strictly compatible with those used in the academic version of CHARMM; however, as the ligand is kept rigid throughout the minimization, they were considered sufficient. The resulting intercalation site was then used in docking simulations to obtain docking energies comparable to those of the insertion studies.

Docking of the optimized structures was performed using AutoDock v 3.0.5,[49] with grid dimensions of 60 × 60 × 40 npts and a grid spacing of 0.375 Å. For the intercalation studies, the grid was centered at the defined intercalation site. In the case of the insertion mode the minor groove was searched between base pairs C2G9 and T8A3. Results of the docking runs comprised molar inhibition constants K_i (or μmolar constants $K_i \times 10^6$), free energies ($\Delta E_i \approx \Delta G_i = -RT \ln K_i^{-1}$) in kcal/mol (see below), and the positioning of the ligand in the receptor.

The usefulness of this approach was tested by investigating the typical minor groove intercalators ethidium and daunomycin as well as the minor groove binder distamycin in the same manner as **1**. Results obtained in this way show that the approach taken should lead to a reasonable description of docked **1** and useful binding energies.

The warhead of **1** is an unusual, highly strained system and as such contains nonstandard bond lengths, angles, and dihedral angles. As the molecule proceeded along the reaction path, the deviation of the warhead geometry from standard structural parameters increased. Such a situation implied that an MM description of the ligand would be inadequate. For the purpose of validating this supposition, we performed a test docking run, with the triggered structure given conformational flexibility, using the Lamarckian Genetic Algorithm (LGA) implemented in AutoDock.[49] As expected, the binding energy decreased by 2.5 kcal/mol, indicating a more stable complex. However, the predicted structure of the triggered molecule in this complex was determined (B3LYP/3-21G calculation) to be 83 kcal/mol less stable than the optimized structure. Thus, as the MM description of **1** was clearly

(39) Frisch, M. J.; et al. *Gaussian 03*, Revision B.05; Gaussian, Inc.: Pittsburgh, PA, 2003.
(40) *SYBYL*; 6.7.1 Tripos Inc.: St. Louis, MO, 63144.
(41) (a) 6-31G(d) or 6-31G(d,p): Hariharan, P. C.; Pople, J. A. *Theor. Chim. Acta* **1973**, *28*, 213. (b) cc-pVDZ: Dunning, T. H., Jr. *J. Chem. Phys.* **1989**, *90*, 1007.
(42) (a) Svensson, M.; Humbel, S.; Froese, R. D. J.; Matsubara, T.; Sieber, S.; Morokuma, K. *J. Phys. Chem.* **1996**, *100*, 19357. (b) Humbel, S.; Sieber, S.; Morokuma, K. *J. Chem. Phys.* **1996**, *105*, 1959. (c) Froese, R. D. J.; Morokuma, K. In *Encyclopedia of Computational Chemistry*; Schleyer, P. v. R., Ed.; Wiley: New York, 1998; p 1244.
(43) Brueckner, K. A. *Phys. Rev.* **1954**, *96*, 508.
(44) Handy, N. C.; Pople, J. A.; Head-Gordon, M.; Raghavachari, K.; Trucks, G. W. *Chem. Phys. Lett.* **1989**, *164*, 185.
(45) *HyperChem*; Hypercube, Inc.: Gainesville, FL 32601.
(46) Cornell, W.; Cieplak, P.; Bayly, C.; Gould, I.; Merz, K.; Ferguson, D.; Spellmeyer, D.; Fox, T.; Caldwell, J.; Kollman, P. A. *J. Am. Chem. Soc.* **1995**, *117*, 5179.
(47) (a) Foloppe, N.; Mackerell, A. D., Jr. *J. Comput. Chem* **2000**, *21*, 86. (b) Mackerell, A. D., Jr.; Banavali, N.; Foloppe, N. *Biopolymers* **2000**, *56*, 257.
(48) Brooks, B. R.; Burccoleri, R. E.; Olafson, B. D.; States, D. J.; Karplus, M. *J. Comput. Chem.* **1983**, *4*, 187.
(49) (a) Momany, F. A.; Rone, R. *J. Comput. Chem.* **1992**, *13*, 888.
(50) Morris, G. M.; Goodsel, D. S.; Halliday, R. S.; Huey, R.; Hart, W. E.; Belew, R. K.; Olson, A. J. *J. Comput. Chem.* **1998**, *19*, 1639.

inadequate (similar observations were made for other force fields), the optimized geometries of receptor and ligand were taken to be fixed throughout the entire docking run.

Since the AutoDock program does not contain fragmental volume or solvation parameters for DNA, the receptor portion of the complex, and as such the full free binding energy calculated by AutoDock was reduced to an intermolecular energy function, which is based on the Weiner force field.[50] The errors made in this way (rigid ligand and receptor lead to an underestimation; the neglect of entropy effects in the docking process lead to an overestimation of the absolute value of the binding energy) were assumed to partially compensate each other, which justified the derivation of K_i from ΔE_i rather than ΔG_i.

The energy function is defined as[51]

$$E_{\text{dock}} = E_{\text{vdw}} + E_{\text{elec}} + E_{\text{HB}} = \Delta E_{\text{vdw}} \sum_{i,j} \left(\frac{A_{ij}}{r_{ij}^{12}} - \frac{B_{ij}}{r_{ij}^{6}} \right) + \Delta E_{\text{HB}} \sum_{i,j} D(t) \left(\frac{C_{ij}}{r_{ij}^{12}} - \frac{D_{ij}}{r_{ij}^{10}} \right) + \Delta E_{\text{elec}} \sum_{i,j} \left(\frac{q_i q_j}{\epsilon r_{ij}^{2}} \right) \quad (2)$$

E_{vdw} incorporates the effects of dispersion and repulsion into the calculation of the binding energy. This term is a parametrized 12−6 Lennard-Jones potential. The E_{HB} term introduces the stabilization that results from the formation of hydrogen bonds and includes a directional weighting factor $D(t)$ with a 12−10 hydrogen-bonding term.[51]

Electrostatic Interactions. The calculation of the electrostatic interaction energy term (E_{elec}) required that the atoms in the complex be assigned a partial charge. In QM/MM calculations it is common to use different charge schemes for ligand (QM description) and receptor (MM description). We tried three different combinations, which had in common that for the receptor component Gasteiger−Hückel charges[52] were assigned throughout using the charge calculation function available in Sybyl.[39] The ligand charges were either Gasteiger−Hückel, Mulliken, or NBO (natural bond orbital) charges,[53] where the latter two charge schemes were taken from the B3LYP/3-21G optimization. Gasteiger−Hückel charges, which lead to binding energies similar to those of the Mulliken charges, fail in the case of the biradical to yield a reasonable charge distribution. Therefore we tested the suitability of Mulliken and NBO charges for the ligand in a comparative docking study for **6**. The Mulliken charges lead to an increased polarity of heteropolar bonds, thus yielding slightly increased charges for heteroatoms, O and N, than was seen from the NBO analysis. This fact was reflected in the binding energy of the two docking attempts, where the molecule with NBO charges had a slightly decreased binding energy for **6** (−6.94 kcal/mol compared to −7.32 kcal/mol). The energy determined by the NBO charges results in a K_i value that is closer to that of experiment (K_i(Mulliken) = 4.34×10^{-6}; K_i(NBO) = 8.25×10^{-6}; K_i(expt) = 2.5×10^{-5} [14]), whereas the alignment of atom C23 with the experimentally predicted H abstraction site is superior for the molecule with Mulliken charges. Thus, we chose the Mulliken charges, as the energy difference between the two methods is within the errors of the approximation and the appropriate binding site is more clearly identified.

Graphical Representation. The embedding of **1** and its follow-up products, into the minor groove of DNA, is presented by the Conolly surface[54] of DNA and the ball-and-stick representation of the drug.

Strain Analysis and Puckering Description. The strain analysis of **1**, compared to **6**, was carried out using the puckering coordinates of rings D, E, and F, which were analyzed with the Cremer−Pople puckering analysis.[55,56] The puckering of a six-membered ring is determined by a superposition of boat/twist-boat forms described by the pseudorotational coordinates q_2 (puckering amplitude) and ϕ_2 (pseudorotational phase angle) and the chair form described by the puckering amplitude q_3. Boat and twist-boat forms span a pseudorotational space of dimension two, whereas the chair form is in the orthogonal one-dimensional inversion space, so that the three-dimensional space of six-membered rings follows. Each conformation in this space is described by the cylindric coordinates (q_2, ϕ_2, q_3) or alternatively by the spherical coordinates $\{Q, \phi_2, \Theta_2\}$ with $Q = \sqrt{q_2^2 + q_3^2}$ and $\Theta_2 = \arctan(q_2/q_3)$. Any puckered six-membered ring can be associated with a point on the conformational globe spanned by the three coordinates, and any six-membered ring conformation can be expressed by a linear combination of the three basis conformations boat, twist-boat, and chair.[56]

The contribution of a basis conformation (or a pair of basis conformations) to the actual conformation observed is given in % according to

$$\%(\text{basis conformation}) = \frac{(q_m)^2}{Q^2} \times 100 \quad (3)$$

where q_m is the corresponding puckering amplitude.[56]

General Considerations. When studying **1**, we made two simplifying assumptions with regard to its properties in the cell environment. (a) Enediyne **1** will be present as an anion at a pH close to 7 (dissociation of a proton at the acetic acid rest $C_{30}O_7O_8H$, Scheme 1).[14] Thus, solvation in aqueous solution will be increased as well as the docking constant. However, since the AutoDock program we used does not possess the solvation parameters for DNA, we excluded the solvation effects and refrained from using the anionic species to limit errors made in this way. (b) It is known that **1** occurs as either the (2*S*,7*R*) or the (2*R*,7*S*) enantiomer, of which only the (2*S*,7*R*) enantiomer is able to correctly bind to the DNA.[7] When the (2*R*,7*S*) enantiomer is docked in the minor groove, it is not able to abstract a H atom from DNA.[7] Hence, in our study, we focused exclusively on the (2*S*,7*R*) enantiomer.

3. Energetic Implications of the Triggering Mechanism of Dynemicin A

In Scheme 2, the possibility is considered that the Bergman cyclization of **1** proceeds directly to **2** via **TS(1−2)**. An activation enthalpy of 52 kcal/mol (B3LYP/6-31G(d)) is calculated for this reaction (Figure 1), which is far too high to lead to any significant formation of biradical **2** at body temperature. The triggering reaction converts **1** into **6** in a strongly exothermic reaction (Figure 1 and discussion below), and the activation enthalpy for **TS(1−2)** is lowered by 34 kcal/mol to that in the case of **TS(6−7)**. The Bergman reaction of **1** is hindered by the existence of an epoxide ring, which causes a drastic increase in the barrier. The major reason for this difference results from the influence of the epoxide ring upon rings D, E, and also F.

The opening of the epoxide in **1** lowers the barrier height of the Bergman reaction of **6**. In the following we have to determine the energy window for the reaction barrier that

(51) Weiner, S. J.; Kollman, P. A.; Case, D. A.; Singh, U. C.; Ghio, C.; Alagona, G.; Profeta, S.; Weiner, P. *J. Am. Chem. Soc.* **1984**, *106*, 765.
(52) Morris, G. M.; Goodsell, D. S.; Huey, R.; Olson, A. J. *J. Comput.-Aided Mol. Des.* **1996**, *10*, 293.
(53) (a) Gasteiger, J.; Marsili, M. *Tetrahedron* **1980**, *36*, 3219. (b) Marsili, M.; Gasteiger, J. *Croat. Chem. Acta* **1980**, *53*, 601. (c) Gasteiger, J.; Marsili, M. *Organ. Magn. Reson.* **1981**, *15*, 353. (d) Streitweiser, A. *Molecular Orbital Theory for Organic Chemists*; Wiley: New York, 1961. (e) Purcell, W. P.; Singer, J. A. *J. Chem. Eng. Data* **1967**, *12*, 235.
(54) (a) Carpenter, J E.; Weinhold, F. *J. Mol. Struct. THEOCHEM* **1988**, *46*, 41. (b) Reed, A. E.; Weinstock, R. B.; Weinhold, F. *J. Chem. Phys.* **1985**, *83*, 735. (c) Reed, A. E.; Curtiss, L. A.; Weinhold, F. *Chem. Rev.* **1988**, *88*, 899.
(55) (a) Connolly, M. L. *Science* **1983**, *221*, 709. (b) Connolly, M. L. *J. Appl. Crystallogr.* **1983**, *16*, 548.
(56) Cremer, D.; Pople, J. A. *J. Am. Chem. Soc.* **1975**, *97*, 1354.
(57) Cremer, D.; Szabo, K. J. In *Methods in Stereochemical Analysis, Conformational Behavior of Six-Membered Rings, Analysis, Dynamics, and Stereoelectronic Effects*; Juaristi, E., Ed.; VCH Publishers: Weinheim, 1995; pp 59−134.

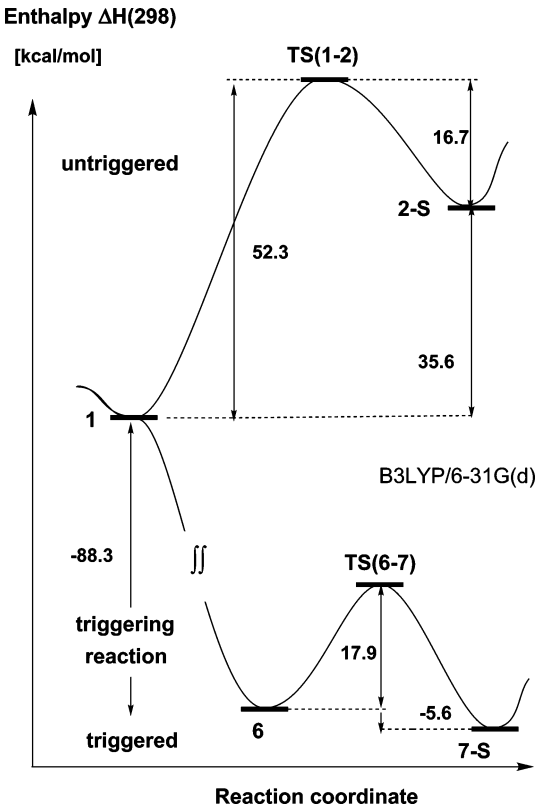

Figure 1. Energy profile for the Bergman cyclization reactions of enediynes **1** and **6**. B3LYP/6-31G(d)//B3LYP/3-21G calculations with B3LYP/3-21G thermochemistry. For numbering compare with Scheme 2.

guarantees biological activity. If there is a large release of strain energy in the triggering reaction, enediyne **6** becomes too stable, the barrier to Bergman cyclization will be too high, and the biological activity of **6** will vanish. However, if the barrier becomes too small, enediyne **6** will convert rapidly to biradical **7S** and the biological activity of the enediyne will last just a short time, which is not desirable from an ADME point of view. Apart from this, the kinetic stability of **7S** will indirectly depend on electronic features that influence the barrier to Bergman cyclization. If this kinetic stability is low (caused, for example, by a low-barrier retro-Bergman reaction to the open enediyne **8**, Scheme 2), the lifetime of **7-S** will be too short for H abstraction from DNA and, consequently, the biological activity of **1** will vanish.

The assessment of the manner in which the strain energy of the epoxide ring tunes the energetics of the reactions of **1** to fit into the allowable energy window was investigated by the role strain release plays in the epoxide ring-opening reaction. In this connection six formal reactions were studied (see Scheme 3) at the B3LYP/6-31G(d)//B3LYP/3-21G level of theory.[57] The energy of reaction 1 defines the conventional ring strain energy of oxirane. This is calculated to be 31 kcal/mol, which is comparable to the experimental value of 27 kcal/mol.[58] If the epoxide ring is part of a bicyclic ring system, as is the case for the monoepoxide of cyclohexadiene (reaction 3), the strain energy decreases by 6.4 kcal/mol to 24.7 kcal/mol (Scheme 3). Actually, reaction 3 is unbalanced insofar as two different alcohols (ethanol and 4-hydroxycyclohexene) are generated in the formal reaction 3. A more balanced reaction is given by reaction 2, as this is formulated parallel to reaction 1 and leads to just 4-hydroxycyclohexene and dimethyl ether. The strain energy is determined, in this case for the monoepoxide of cyclohexadiene, to be 28.8 kcal/mol.

In reaction 2 one has to balance the number of six-membered rings on both sides of the reaction, which implies that cyclohexene rather than ethane is used as a reference. The corresponding reaction for **1** is given by reaction 6 (Scheme 3), which requires the calculation of one additional compound possessing the framework of **1**, albeit without the epoxide ring. To avoid costly additional calculations, the energy of reaction 6 was evaluated by calculating directly the reaction energy of reaction 5, which parallels reaciton 3, and then using the normalization reaction 4 to adjust the reaction energy of reaction 5 to that of 6. In this way, the reaction energy (6) was determined to be −22.2 kcal/mol (Scheme 3).

Since there is no reason to assume that the epoxide **1** is less strained than a normal epoxide, it is obvious that the alcohol **6** is 9 kcal/mol more strained than a normal alcohol. Considering the experimental value for the strain energy of oxirane (27 kcal/mol,[58] thus giving an error of 4 kcal/mol for the calculation), one can predict that 18 kcal/mol (= −22.2 + 4) are set free in the epoxide ring-opening reaction leading from **1** to **6**. This is accompanied by the formation of two new bonds (C8−H and O1−H), which add to the energy gain, as will be discussed below. Hence, the resulting alcohol **6** is significantly stabilized, although there is still some residual strain stored in ring F, which is caused by the nonlinear arrangement at the triple bonds. This residual strain is responsible for the fact that the activation enthalpy for the Bergman reaction, resulting therefrom (16.7 kcal/mol, Figure 1 and below), fits exactly into the energy window needed for the generation of the biradical **7-S** (instead of **2-S**) under physiological conditions.

Enediyne **1** is activated by reducing agents such as nicotinamide adenine dinucleotide phosphate (NADPH), thiols, other reducing agents, or visible light.[5b] The triggering reaction is initiated by a one- or two-electron reduction of **1** to yield the hydroquinone, **4** (see Scheme 2), which rearranges through the epoxide opening to the semiquinone methide, **5**. Then, by protonation, the quinone alcohol (**6**) is formed, which is the starting product for the Bergman cyclization reaction. Although chemically this process seems to be clear,[5b] its steric consequences for the Bergman reaction still have to be clarified. For this purpose, we will describe the changes in the puckering of rings D, E, and F using the Cremer−Pople puckering analysis.[55,56]

In Table 1, the ring puckering coordinates of D and E are given for the crystal structure of deoxy-dynemicin A,[4] **1**, **6**, **TS-(6−7)**, and **7**. They provide a quantitative measure, contracted into just a few numbers rather than 3*N* Cartesian coordinates or *N* dihedral angles (*N*: size of the ring), of how the calculated overall shape of these rings compares with the corresponding experimental data and how the ring conformations change in the epoxide opening and along the Bergman reaction path. The conformations of rings D and E of **1** closely resemble those of deoxy-dynemicin A.[4] The puckering coordinates reveal in addition that the epoxide ring forces rings D and E into specific conformations, which are more of a boat/half-boat (envelope)

(58) Ahlström, B. Diploma Thesis, Göteborg, 2001
(59) (a) Cremer, D.; Kraka E. *J. Am. Chem. Soc.* **1985**, *107*, 3800. (b) Cremer, D.; Kraka, E. In *Molecular Structure and Energetics*; Liebman, J. F., Greenberg, A., Eds.; VHS Publishers: Deerfield Beach, 1988; Vol. 7, p 65.

Scheme 3. Determination of the Strain Energy of **1** Relative to that of **6** According to B3LYP/6-31G(d)//B3LYP/3-21G Calculations[a]

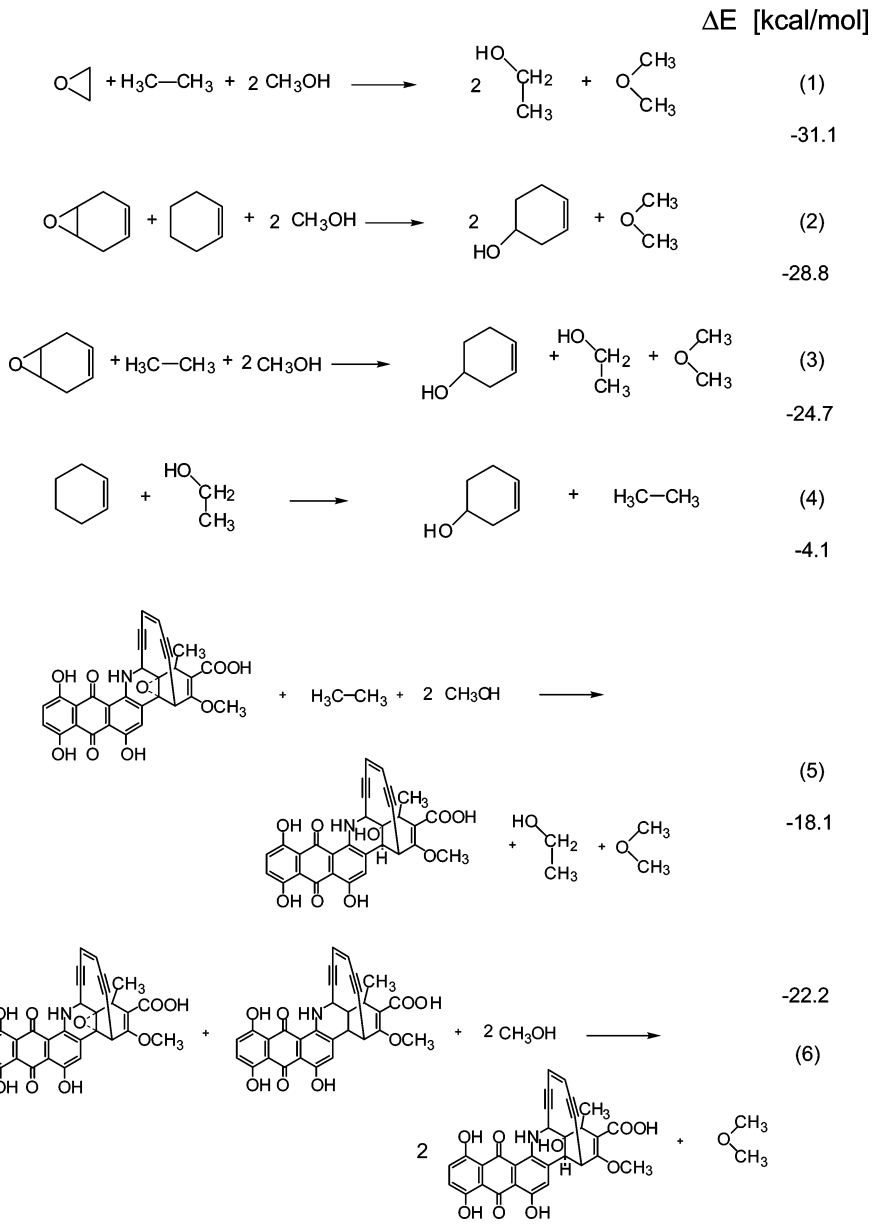

[a] Molecular geometries and energies of the reference molecules are given in the Supporting Information. 4-Hydroxycyclohexene was found to be more stable with the OH group in an equatorial position (Q = 0.509 Å; ϕ_2 = 26.5°; Θ_2 = 129.6°; see Supporting Information).

type (ring D) or the boat/twist-boat type (ring E) rather than the half-chair type conformation of unstrained cyclohexene, which is clearly documented by the puckering coordinates listed in Table 1.

The conformations of rings D and E are a direct consequence of the epoxide, which enforces a boat/half-boat or boat/twist-boat conformation, as a half-chair conformation would lead to twisting of the epoxide ring and consequently a strong increase in the strain energy. As soon as the epoxide is cleaved and an alcohol is formed, this constraint no longer exists. Thus, rings D and E can adopt larger puckering amplitudes and increased half-chair or twist-boat character (Table 1), as is documented in detail in the Supporting Information.

Since ring E obtains more twist-boat character, which is possible because the epoxide ring is no longer hindering this, the carbon atoms, being a part of the 10-membered ring, can stick more out of the plane of the ring system, D−E, and as such, shorten the distance that has to be bridged by the enediyne unit. This is directly reflected by distance C2−C7, which in the epoxide form **1** is equal to 3.815 Å but becomes 3.619 Å as soon as the epoxide opens up. A number of consequences result for the enediyne unit, as follows.

The 10-membered ring F, including the enediyne unit, has in **1** a total puckering amplitude of 0.712 Å and in **6** a total puckering amplitude of 0.652 Å. The puckering analysis reveals that centers C23 and C28 move closer together because of the epoxide ring opening. The through-space distance C23−C28 is 3.540 Å in **1**, however decreases by 0.371 Å to 3.169 Å in **6**. Hence, the increase in puckering of the two six-membered rings D and E, accompanying epoxide opening, leads to changes in the conformation of the 10-membered ring F. These changes facilitate bond formation between center C23 and C28 and, by this, the Bergman cyclization reaction. We note that nature has built a very simple locking−unlocking principle: A single

Table 1. Conformational Analysis of Rings **D** and **E**[a]

molecule	method	ring	Q	q_2	ϕ_2	q_3	Θ
deoxy-dynemicin A	X-ray	D	0.426	0.372 (76)	346.0	0.208 (24)	119.2
		E	0.371	0.369 (99)	134.2	0.037 (1)	84.3
1	B3LYP/3-21G	D	0.427	0.398 (87)	357.0	0.154 (13)	111.1
		E	0.413	0.407 (97)	133.0	0.072 (3)	79.9
6	B3LYP/3-21G	D	0.458	0.392 (73)	15.3	0.237 (27)	121.2
		E	0.532	0.518 (95)	143.9	0.120 (5)	77.0
TS(6−7)	B3LYP/3-21G	D	0.507	0.397 (61)	48.3	0.316 (39)	128.6
		E	0.527	0.443 (71)	174.1	0.285 (29)	57.2
7-S	B3LYP/3-21G	D	0.536	0.424 (63)	46.5	0.327 (37)	127.6
		E	0.566	0.484 (73)	168.9	0.293 (27)	58.8

[a] The crystal structure data of deoxy-dynemicin A are taken from ref 4. The puckering amplitudes (Q, q_m) are given in Å, the pseudorotational phase angles ϕ_2 and the polar angle Θ are in degrees. Boat conformations are found at $\phi_2 = 0 = 360$, 60, 120, 180, 240, 300°, twist-boat conformations at $\phi_2 = 30$, 90, 150, 210, 270, 330°. The values in parentheses denote the character of boat/twist-boat (q_2) or chair (q_3) conformation in percentage. Polar angle Θ indicates whether a conformation is more in the equator plane (Θ close to 90°) or closer to the poles (Θ close to 0 or 180°) of the conformational globe.[53]

epoxide lock can, when opened, change conformation and strain in the two rings D and E, which regulate the flexibility of ring F.

4. Energetics of Bergman and Retro-Bergman Cyclization of Dynemicin A

There are two important considerations in the Bergman cyclization reaction of dynemicin A. First, is the activation barrier sufficiently low such that the reaction takes place at physiological conditions? Second, is the product kinetically stable to allow the abstraction of H atoms, which requires an activation energy of 10−12 kcal/mol,[59] from DNA? In Table 2, the enthalpies $\Delta H(298)$ and free energies $\Delta G(298)$ calculated at the B3LYP/3-21G, B3LYP/6-31G(d), and ONIOM(BD(T)/cc-pVDZ;B3LYP/3-21G) levels of theory along the reaction path **6** → **7** → **8** (Scheme 2) are listed.

All calculations predict that the triggered enediyne, **6**, has a Bergman activation enthalpy that is more than 30 kcal/mol smaller than that of **1** and, by this, low enough to undergo the Bergman cyclization at body temperature. The DFT calculations suggest $\Delta H^a(298)$ values of 17.6 and 17.9 kcal/mol, whereas BD(T) leads to a lower value of just 13.5 kcal/mol (Table 2). We note that for the parent enediyne (3-hexen-1,5-diyne, **11**) B3LYP/3-21G and CCSD(T) lead to the same energetics within 1 kcal/mol, whereas BD(T)/cc-pVDZ values at B3LYP/3-21G geometries underestimate the activation enthalpy by 2.7 kcal/mol. In Table 3, the errors of the three methods used in this work are given for the parent enediyne **11**, where as reference the experimental results[60] corrected to 298 K[28] are given. Using these values as corrections and averaging over the three calculations, the most likely value is derived to be (16.9 + 17.1 + 16.2)/3 = 16.7 kcal/mol (Table 3). Hence, the triggered enediyne **6** can react with a sufficiently large rate at body temperature to become biologically active.

The Bergman reaction of **6** is predicted to be exothermic according to calculated $\Delta H_R(298)$ values of −2.5, −5.6, and −6.2 kcal/mol (best value: −2.6 kcal/mol, considering corrections of 0, −4.9, and −1.5 kcal/mol for the parent enediyne **11**; Table 3, Table 2, and Figure 2). The exothermicity of the cyclization reaction decides on the possibility of a retro-Bergman reaction to **6**, which requires 19.7, up to 23.5, kcal/mol (best value 19.4 kcal/mol) and therefore should not play a significant role under physiological conditions. The same is true for the retro-Bergman reaction leading from **7-S** to enediyne **8**. The activation enthalpy is predicted to be between 20.3 and 25.6 kcal/mol (Table 2; most likely value 21.6 kcal/mol) at body temperature.

Actually, open enediyne **8** can be related to the parent enediyne **11** because both are unstrained in the enediyne part and both possess therefore the same activation enthalpy of 29 ± 1 kcal/mol (**11**: $\Delta H^a(298) = 28.2$ kcal/mol;[28,60] see Table 3). Also the reaction enthalpy of the Bergman cyclization of **8** is similar to that of **11** ($\Delta H_R(298) = 8.0$ kcal/mol compared to 8.5 kcal/mol, Table 3;[28,60] in this case B3LYP/3-21G turns out to be very accurate due to a cancellation of errors[19]). Accordingly, the enthalpy difference between the two isomers **6** and **8** provides a good measure for the strain invoked by ring F. This is about 11 kcal/mol (Table 3), which together with the data in Scheme 3 explains the changes in the energetics caused by the triggering. The stability of the ring systems D and E in **1** is raised by about 30 kcal/mol (opening of the epoxide ring), which is reduced by 10.8 ≈ 11 kcal/mol due to the increase in strain energy for ring F (flattening of the ring combined with a contraction along the line C23−C28 and a stronger bending of the linear triple bond units). The latter strain is relieved in **TS(6−7)**, which means that enediyne **6** gains a stabilization of 22 kcal/mol relative to **1** (Scheme 3). However, it is still destabilized by 11 kcal/mol, relative to **TS(6−7)**, and as such leads to a lowering of the Bergman cyclization activation enthalpy from 28 to about 17 kcal/mol.

We are now in the position to determine the enthalpy window, which guarantees that the Bergman cyclization will occur with sufficient rate and the resulting intermediate biradical, **7-S**, will have a sufficient kinetic stability (long enough lifetime) for the H abstraction to occur. For a chemical reaction to proceed by 50% at body temperature ($T = 310$ K) within 5 min or faster, the free activation enthalpy, $\Delta G^a(310)$, has to be 22 kcal/mol or lower. In the case of the Bergman reaction of **6** the activation entropy is −4.7 entropy units (Table 2; for **11** it was measured to be −7 eu[60]). Therefore, the activation enthalpy $\Delta H^a(310)$ has to be 23.5 kcal/mol or lower. The activation enthalpy for H abstraction from methanol, by *para*-benzyne (**12**), is calculated to be 10−12 kcal/mol.[59] Accordingly, the lower barrier for the window is set to be 11.2 kcal/mol; that is, if the activation enthalpy of the retro-Bergman reaction is smaller than 14 kcal/mol (**7-S** is stabilized by 2.8 kcal/mol below **6**), the kinetic stability of the biradical will be too low to guarantee H abstraction from DNA. The calculated activation enthalpy of **6**

(60) Kraka, E.; Cremer, D. To be published.
(61) Roth, W. R.; Hopf, H.; Horn, C. *Chem. Ber.* **1994**, *127*, 1765.

Table 2. Energetics of the Bergman Reaction of Triggered Dynemicin A **6**[a]

molecule	R/U	ref	E, ΔE	ZPE	H(298), ΔH(298)	S(298)	G(298), ΔG(298)	μ
				B3LYP/3-21G				
6	R		−18767.11903	288.6	−1876.62701	195.9	−1876.72008	4.4
TS(6−7)	R	**6**	19.4	287.4	17.6	191.2	19.0	4.2
7-S	BS-U	**6**	−2.1	288.8	−2.5	190.8	−1.0	4.9
7-T	U	**7-S**	2.8	289.0	3.0	193.5	2.2	5.0
TS(7−6)	R	**7-S**	21.5		20.1		20.0	
TS(7−8)	R	**7-S**	22.4	286.4	20.3	191.9	20.0	5.4
8	R	**7-S**	−8.5	287.0	−9.1	198.6	−11.4	4.7
TS(8−7)	R	**8**	30.9		29.4		31.4	
8	R	**6**	−10.6		−11.6		−12.4	
				B3LYP/6-31G(d)//B3LYP/3-21G				
6	R		−1887.44774		−1886.95572[b]		−1887.04879[b]	4.4
TS(6−7)	R	**6**	19.7		17.9		19.3	4.2
7-S	BS-U	**6**	−5.2		−5.6		−4.1	5.0
7-T	U	**7-S**	2.2		2.4		1.6	5.1
TS(7−6)	R	**7-S**	25.0		23.5		23.4	
TS(7−8)	R	**7-S**	27.7		25.6		25.3	5.4
8	R	**7-S**	−2.9		−3.5		−5.8	4.7
TS(8−7)	R	**8**	32.9		31.2		29.4	
8	R	**6**	−8.1		−9.1		−9.9	
				BD(T)/cc-pVDZ;B3LYP/3-21G//B3LYP/3-21G[c]				
6	R		−1877.73138		−1877.23936[b]		−1877.33243[b]	4.4
TS(6−7)	R	**6**	15.3		13.5		14.9	4.2
7-S	BS-U	**6**	−5.8		−6.2		−4.7	5.0
7-T	U	**7-S**	3.6		3.8		3.0	5.1
TS(7−6)	R	**7-S**	21.1		19.7		19.6	
TS(7−8)	R	**7-S**	23.0		20.9		20.6	5.4
8	R	**7-S**	−4.3		−4.9		−7.2	4.7
TS(8−7)	R	**8**	27.3		27.1		25.3	
8	R	**6**	−10.1		−11.11		−11.9	

[a] Absolute energies and enthalpies in hartrees, relative energies, zero-point energies (ZPE), and relative enthaplies in kcal/mol, entropies in cal/(mol·K), and dipole moments in Debyes. For the numbering of compounds compare with Scheme 2. R, U, BS-U indicate whether restricted (R), unrestricted (U), or broken-symmetry unrestricted (BS-U) DFT was used where the application of the latter was a result of an external instability of RDFT. Notations such as **TS(6−7)** and **TS(7−6)** refer to the same TS, however indicate that relative energies are given with regard to different references. Ref denotes that molecule that is used as a reference for calculated energy (enthalpy) differences ΔE (ΔH, ΔG). The imaginary frequency of the transition state **TS(7−8)** is 459i, and that of **TS(7−8)** is 489i cm^{-1}. [b] The thermochemical corrections of the B3LYP/3-21G calculations were used. [c] ONIOM calculations using a BD(T) description of the warhead (6 carbon and 2 hydrogen atoms) and a B3LYP/3-21G description of the remainder of the molecule. For **7-S** and **7-T** UBD(T) was used.

Table 3. Best Available Data for the Bergman Cyclization of Some Enediynes[a]

	enediyne **11**		
		errors	
enthalpy	value expt[b]	B3LYP 3-21G	B3LYP 6-31G(d)	BD(T) cc-pVTZ
ΔH^a(**11**−**12**)	28.2 ± 0.5	0.7	0.8	−2.7
ΔH_R(**11**−**12**)	8.5 ± 0.5	0	−4.9	−1.5
ΔH^a(**12**−**11**)	19.7 ± 0.5	0.7	5.7	−1.2
$\Delta H(S - T,$ **12**)	3.5	−0.3	−1.1	−2.0[c]

enediyne **6**			enediyne **8**		
enthyalpy	gas	DNA	enthalpy	gas	DNA
ΔH^a(**6**−**7**)	16.7	17.9	ΔH^a(**8**−**7**)	29.8	29.8
ΔH_R(**6**−**7**)	−2.6	−3.0	ΔH_R(**8**−**7**)	8.0	8.4
ΔH^a(**7**−**6**)	19.4	21.0			
$\Delta H(S - T,$ **7**)	3.4	3.4			
ΔH^a(**7**−**8**)	21.8	22.0	ΔH_R(**6**−**8**)	−10.6	−10.3

[a] Activation enthalpies ΔH^a, reaction enthalpies ΔH_R, and singlet−triplet splittings $\Delta H(S - T)$ in kcal/mol at 298 K. Gas denotes calculated values for the gas phase, and DNA calculated values for the DNA−enediyne complex. Notations such as **TS(11**−**12)** and **TS(12**−**11)** refer to the same TS, however indicate that relative energies are given with regard to the forward and backward reaction, respectively. [b] From refs 60 and 61. [c] Value not used.

(16.7 kcal/mol, Table 3) is in the lower half of the enthalpy window from 11.2 to 23.5 kcal/mol, thus suggesting high biological activity.

The biological activity of **1** is based on two stereochemical facts. An epoxide ring induces so much strain that in the untriggered form the Bergman cyclization becomes impossible at body temperature. The enediyne unit is incorporated into a 10-membered ring bridging rings D and E, which (a) reduces the critical C23−C38 distance from 3.54 to 3.17 Å after triggering and (b) increases, by (a), the strain of the enediyne ring F by 11 kcal/mol so that the Bergman cyclization barrier is reduced to 16.7 kcal/mol. Furthermore, the biradical **7-S** is

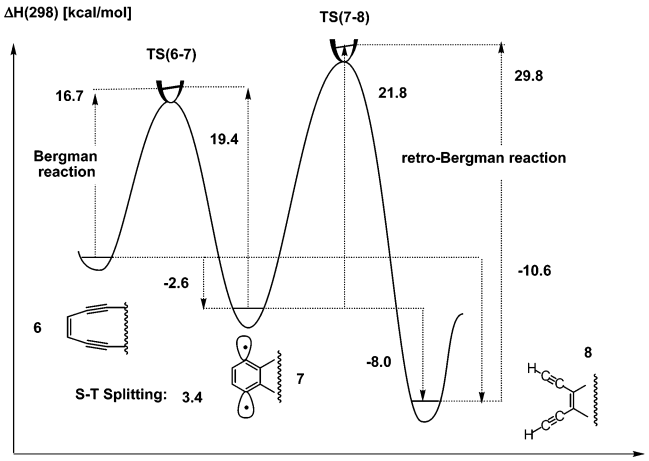

Figure 2. Enthalpy profile for the Bergman cyclization of triggered dynemicin **6** according to the best data obtained in this work (see Table 3).

kinetically stable, as shown by the retro-Bergman activation enthalpies of 19.5 and 21.8 kcal/mol, respectively (Table 3).

Previously, we have estimated the reactivity of the biradical by its singlet−triplet (S−T) splitting.[29a,30] If this is relatively large (up to 5 kcal/mol), the singlet will not be very reactive. On the contrary, if it is relatively small (down to 1 kcal/mol), the singlet biradical will be highly reactive. For the parent biradical *para*-benzyne (**12**) a S−T splitting of 3.5 kcal/mol (Table 3) was found.[61] A similar value is calculated for **7** (3.0, 2.4, 3.8 kcal/mol, Table 2; most likely value is 3.5 kcal/mol, Table 3), which suggests that biradicals **7-S** and **12-S** possess the same H abstraction ability. Thus, the H abstraction barriers calculated for **12-S** are also valid for **7-S** (see above).

5. Docking of Dynemicin A in the Minor Groove of DNA

Natural enediyne **1** has been identified as a minor groove intercalator[6−16] similar to many other compounds with an anthraquinone or an anthraquinone-similar unit.[62−67] For the intercalation to occur, the separation between two base pairs must be widened from 3−4 to about 7−8 Å to accommodate the ligand. In this work, this was done for the sites between base pairs A9T2 and T8A3, T8A3 and G7C4, A6T5 and T5A6, and T5A6 and G4C7. After intercalation of **1** the geometry of DNA was reoptimized to adjust the opening between the base pairs to the intercalator size. During this procedure the ligand was frozen at the DFT geometry. For reasons of comparison, this procedure was repeated for two typical intercalators, daunomycin[68] and the ethidium cation,[62b] and the minor groove binder distamycin.[69] Results of the intercalation studies are listed in Table 4.

Intercalation between two base pairs can be considered as an induced fit process; that is, the receptor has to be deformed to host the ligand. The energy to form the required cavity provides a reasonable approximation for the activation energy of the intercalation process. Using the procedure described above, we calculate cavity energies of 23.4 kcal/mol for forming the intercalation site between A9T2 and T8A3 (opening from 3.4 to 7.9 Å), 16.9 for T8A3 and G7C4 (7.0 Å), 19.4 for A6T5 and T5A6 (7.5 Å), and 22.4 kcal/mol for T5A6 and G4C7 (7.1 Å), thus suggesting activation energies between 17 and 23 kcal/mol. Kinetic measurements have suggested that the activation free energy for intercalation of a typical intercalator such as proflavin is about 15 kcal/mol.[70] So far, none of the MD simulations reported in the literature have been able to lead to a reasonable activation energy for intercalation.[64] Considering the height of the barrier, it is clear that intercalation is a dynamic process that requires much longer simulation times than nanosecond-MD simulations. From the data we obtained it can be concluded that the activation energies for intercalation and for the Bergman reaction are comparable.

As shown in Table 4, the calculated binding free energies ΔG for the ethidium cation and daunomycin are exaggerated by 54 and 74%, which is in line with the results made by other authors. It is also not surprising that the intercalation binding energies for **6** are larger by 49−123% than the experimental value given by Myers and co-worker ($\Delta G = -6.45$ kcal/mol[14]). In the literature[62−64] researchers have speculated about this exaggeration of intercalation energies considering the various approximations made in the calculation. We note that the exaggeration may have less to do with force field and other technical ingredients of the calculation. It simply results from the fact that a rigid, rather than a dynamic model of B-DNA has to be used in the calculations. Intercalations will take place until each favorable intercalation position is occupied and an equilibrium between deintercalating and intercalating molecules is established. In this situation B-DNA is partly unwound and stretched. Activation and binding energies for intercalation will be smaller than those calculated for a rigid B-DNA molecule.

We used the intercalation model for **6** and B-DNA to explain a number of experimental observations.

(1) The intercalation model explains the effect of the hydroxyl groups O4H and O6H at ring A (Scheme 1). Myers and co-workers[14] found that the measured binding free energy for intercalation decreases by 2.5 kcal/mol from 6.5 to just 3.8 kcal/mol when replacing these OH groups with H atoms. In our calculations, we found a decrease by 1.2 kcal/mol. Figure 3b reveals that the OH groups of ring A stick out into the major groove, where they can be fixed by H-bonding with water molecules. In this way, the OH groups increase the intercalation binding energy because additional energy is needed to free the OH bonds from H-bonding.

(2) The intercalation model clarifies also the role of the COOH group. In aqueous solution, the COOH group forms the COO anion, which is strongly solvated. If the anion is converted into an ester, the binding energy for intercalation increases by 2.6 to 3 kcal/mol (without and with OH groups at ring A).[14] Two reasons are responsible for this increase. (a) In the

(62) Wenthold, P. G.; Squires, R. R.; Lineberger, W. C. *J. Am. Chem. Soc.* **1998**, *120*, 5279.
(63) (a) Ren, J.; Chaires, J. B. *Biochemistry* **1999**, *38*, 16067. (b) Ren, J.; Jenkins, T. C.; Chaires, J. B. *Biochemistry* **2000**, *39*, 8439.
(64) Cashman, D. J.; Kellogg, P. A. *J. Med. Chem.* **2004**, *47*, 1360.
(65) Trieb, M.; Rauch, C.; Wibowo, F. R.; Wellenzohn, B.; Liedl, K. R. *Nucl. Acids Res.* **2004**, *32*, 4696.
(66) Baraldi, P. G.; Bovero, A.; Fruttarolo, F.; Preti, D.; Tabrizi, M. A.; Pavani, M. G.; Romagnoli, R. *Med. Res. Rev.* **2004**, *24*, 475.
(67) Snyder, R. D.; Ewing, D. E.; Hendry, L. B. *Environ. Mol. Mutagen.* **2004**, *44*, 163.
(68) Armitage, B.; Changjun, Y.; Devadoss, C.; Schuster, G. B. *J. Am. Chem. Soc.* **1994**, *116*, 9847.
(69) Chaires, J. B.; Priebe, W.; Graves, D. E.; Burke, T. G. *J. Am. Chem. Soc.* **1993**, *115*, 5360.
(70) Chaires, J. B. *Biopolymers* **1997**, 201.
(71) (a) Li, H. J.; Crothers, D. *J. Mol. Biol.* **1969**, *39*, 481. (b) Nuss, M. E.; Marsh, F. J.; Kollman, P. A. *J. Am. Chem. Soc.* **1979**, *101*, 825, and in ref 64.

Table 4. Calculated Docking Energies ΔE_b Obtained for Different Ligands and Different Docking Modes[a]

structure	docking mode	docking site	ΔE_b	next H to C24	distance	next H to C27	distance
6	intercalation	A9T2-T8A3	−9.6	A9H5	3.256	C4H5	7.771
		T8A3-G7C4	−11.1	C4H5	3.793	A9H5	5.276
		A6T5-T5A6	−14.4	A6H5	4.206	G7H5	6.463
		T5A6-G4C7	−14.1	C7H5	4.339	A6H5	5.835
TS(6−7)	intercalation	A9T2-T8A3	−11.6	A9H5	3.165	C4H5	8.243
		T8A3-G7C4	−13.8	T8H5	3.468	A6H5	4.106
		A6T5-T5A6	−14.5	A6H5	4.347	G7H5	6.061
		T5A6-G4C7	−15.4	T5H5	2.644	G9H5	4.360
7-S	intercalation	A9T2-T8A3	−13.4	A9H5	3.135	C4H5	7.905
		T8A3-G7C4	−12.6	T8H5	3.227	A6H5	3.499
		A6T5-T5A6	−14.8	A6H5	4.633	G7H5	6.082
		T5A6-G4C7	−15.3	C7H5	3.731	G7H5	5.640
ethidium	intercalation	A6T5-T5A6	−10.3 (−6.7)				
daunomycin	intercalation	A6T5-T5A6	−13.7 (−7.9)				
ethidium	insertion	A9T2-C2G9	−9.2				
daunomycin	insertion	A9T2-C2G9	−7.6				
distamycin	insertion	A9T2-C2G9	−8.2 (−10.1)				

[a] Orientation in the docking site and docking energies obtained with AutoDock, and minimization of the intercalation site performed with CHARMM as described in Section 2 of the text. Energy differences in kcal/mol, distances in Å. For the numbering of C atoms, see Scheme 1. The labeling of base pairs is given in Figure 3. Experimental binding free energies ΔG are given in parentheses: ethidium cation, ref 62b; daunomycin, ref 68; distamycin, ref 69.

intercalation mode the COO group sticks out into the minor groove (Figure 3), where the anion is positioned between the negatively charged phosphate groups, which leads to destabilization. A methyl ester at ring E, however, reduces electrostatic repulsion. (b) In addition, it can establish H-bonds with the DNA backbone. This is not possible for the COO anion because it is surrounded by a solvent shell.

(3) The strongest argument for the intercalation model arises from the fact that binding energies above 9 kcal/mol make derivatives of **1** biologically inactive, again documented by results of Myers and co-workers.[14] Considering the fact that the activation energy for intercalation is about 15 kcal/mol or even higher, the barrier for leaving the intercalation site in the case of strong binding would be 24 kcal/mol or higher; that is, this process would be too slow at room temperature to lead to any free **1**, once it is intercalated.

(4) The intercalation model explains why typical intercalators with large binding energies suppress the biological activity of **1**. An intercalator such as daunomycin occupies the most favorable intercalation site and hinders **1** to intercalate because its binding free energy (exptl value −7.9 kcal/mol,[68] Table 4) is 1.4 kcal/mol larger in magnitude than the value of **1** (−6.5 kcal/mol[14]) so that the equilibrium between intercalating molecules is shifted by about 90%.

(5) A typical minor groove binder such as distamycin also suppresses the biological activity of **1**.[6] Distamycin has an experimental minor groove binding free energy of −10.1 kcal/mol,[69] which is 2 kcal/mol larger in magnitude than the value we calculate (−8.2 kcal/mol, Table 4). Distamycin blocks the whole minor groove for **1** to enter. Any strong minor groove binder should have the same effect on **1** as distamycin.

There are however also some facts that speak against intercalation as the necessary step for **1** to develop its biological activity, as follows.

(a) The intercalation of the anthraquinone unit between the base pairs removes the possibility of triggering **1** (see Figure 3). This was also emphasized by other authors. Schuster and co-workers[67] assume an equilibrium between intercalated and nonintercalated structures to make a triggering of **1** outside the minor groove possible. Clearly, for leaving the intercalation site **1** has to surmount an activation barrier of 6.5 + 15 = 21.5 kcal/mol, which is still possible at room/body temperature, but is far too slow to lead to a significant amount of nonintercalated **1**. In this connection one has to consider the unwinding and stretching of DNA, which will facilitate deintercalation. Considering that the latter process is no longer possible for a binding energy of −9 kcal/mol,[14] one can conclude that the barrier is reduced for **1** from 21 to at least 18 kcal/mol, thus allowing some dynemicin molecules to deintercalate.

(b) By intercalating the consecutive structures **6**, **TS(6−7)**, and **7**, we find that in none of the four intercalation modes will the biradical **7-S** be in a position to abstract a H′ atom from the DNA backbone. The distances between the radical centers and the H′ atoms are all larger than 3 Å (Table 4). The target H atom G7-H5′ does not get closer to the radical centers than 5.6 Å. The warhead is positioned in the middle of the minor groove, and this position is ineffectual for the purpose of abstracting a H atom from the DNA backbone. It is generally known that B-DNA becomes unstable when proteins or genes dock to the double strands so that strong bends or even kinks occur.[71] There may be also some instability of B-DNA when relatively small molecules occupy the various intercalation sides. Attempts to model this situation by unwinding and stretching the duplex used in this work did not indicate that the enediyne (biradical) part can easily abstract the G7-H5′ atom. We conclude that H abstraction is difficult for intercalated **7-S**. A previous MD study on this point[72] has indicated that in the case of **6**, for which the alignment is actually much better than for **7-S** (Figures 3c and 3d), a nonnegligible barrier exists that hinders the movement of the ligand toward the abstraction site. In this work, we calculated a barrier larger than 20 kcal/mol for a rotation of **7-S**.

We conclude that **1** once intercalated cannot be triggered. If **1** is triggered to form **6** before it intercalates, it can undergo the Bergman reaction in the intercalation mode. For the different intercalation possibilities, we calculate activation enthalpies of 16.7 − 2.0 = 14.7, 14.0, 16.6, and 15.3 kcal/mol (using the

(72) Travers. A. A.; Thompson, J. M. T. *Philos. Trans. Soc. London A* **2004**, *362*, 1265.
(73) Hopfinger, A. J.; Cardozo, M. G.; Kawakami, Y. *J. Chem. Soc., Faraday Trans.* **1995**, *91*, 2515.

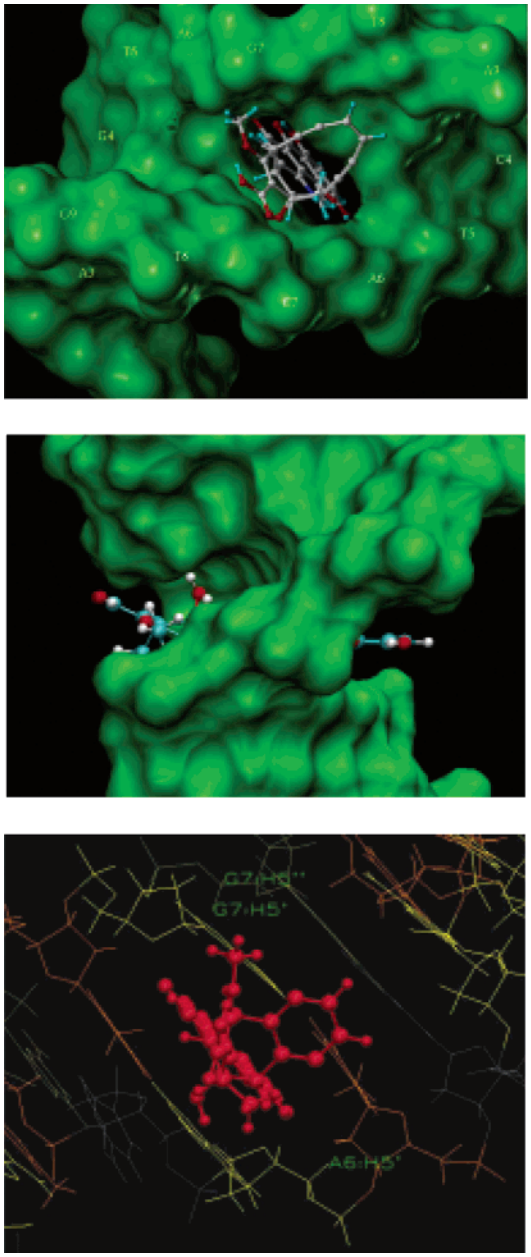

Figure 3. Intercalation modes of various dynemicin structures. (a) Enediyne **1** intercalated between base pairs A6T5 and T5A6. DNA is presented by a Conolly surface. Front view. (b) The same as part a, but side view. One of the OH groups at ring A can be seen to stick out into the major groove. (c) Biradical **7-S** intercalated between base pairs A6T5 and T5A6. DNA is given in a wireframe representation to recognize base pairs and the H atoms next to the biradical centers.

changes in binding free energies of Table 4). However, in none of the intercalation modes is it possible to abstract H atom G7-H5′ without a considerable additional barrier. Considering this result in connection with point 3 above (biological inactivity of strong intercalators), we suggest an insertion−intercalation model that resolves problems a and b.

As part of the recognition step, **1** inserts edgewise into the minor groove (see Figure 4a) and forms an intermediate complex, from which it can proceed to get into the intercalation position. This is done by first positioning ring A between two base pairs (H-bonds and electrostatic interactions play a role in this connection), then ring E and the enediyne bridge swing out (driven by repulsion between the COO anion and negative phosphate groups), and **1** intercalates head-on between two base pairs. In the reverse way, **1** can move into the minor groove and stay in the minor groove in the inserted mode before dissociating. Hence, we assume an equilibrium between insertion and intercalation mode. We note in this connection that a similar mechanism for intercalation has been suggested for a ruthenium complex that intercalates via the major groove.[73]

For the purpose of testing this hypothesis, we investigated the insertion of **1** into the minor groove area between base pairs A9T2 and C2G9 (Table 5). The insertion mode does not lead to any significant distortion of DNA and therefore proceeds without a docking barrier. It follows a lock and key principle rather than an induced fit procedure as in the intercalation mode. The most favorable insertion positions were determined for **1**, **6**, **TS(6−7)**, and **7-S** again employing the AutoDock routine. On average, each docking run resulted in four distinct clusters, corresponding to four different insertion alternatives for the molecule under consideration. In each case, the best docked structure was chosen from the cluster according to the following three requirements: (a) the binding energy ΔE has to be maximal to guarantee a stable insertion complex; (b) it must be possible that H atom G7-H5′ can be abstracted as identified in the experimental study;[6] (c) the overall orientation of enediyne **1** within the minor groove should remain consistent throughout the Bergman reaction.

Criteria a−c were satisfied for only one of the possible orientations in the minor groove, which is shown in Figure 4 for the untriggered form **1**. The molecule is inserted in a parallel fashion along the minor groove, with the atom N1 (Scheme 1) pointing outward and the warhead toward the T5A6G7 trinucleotide sequence. The calculated binding energy is −7.6 kcal/mol for **1** and −7.3 kcal/mol for **6**, which clearly indicates that insertion leads to a stable complex, but is not the energetically favored docking mode. As discussed above, intercalation energies are exaggerated, whereas in the insertion mode binding energies are sometimes overestimated in magnitude (calicheamicin; by −2.8 kcal/mol[59]), and sometimes underestimated in magnitude (distamycin: −8.2 (calculated) vs −10.1 kcal/mol (measured), Table 4) depending on the interactions of the minor groove binder with DNA. In the present case, we estimate a docking energy for inserted **1** of −4.7 to −5 kcal/mol depending whether a correction of 2.8 kcal/mol (calicheamicin) or an exaggeration factor of 1.5 is assumed.

The insertion of **1** occurs in such a way that the dynemicin pro-radical carbon atom (C27) is aligned with the H5′ atom of the G7 residue (r(CH) = 2.707 Å, **1**, Table 5), which according to experimental findings[6] is the preferred abstraction site for this sequence.

The orientation of **1** in the minor groove can be rationalized by considering the global shape of the molecule, which resembles that of a sickle (Scheme 4). If the opening of the sickle is oriented toward the interior of the minor groove (situation a in Scheme 4, compare also with Figure 4b), there will be more stabilizing docking interactions than in the situation in which the opening is pointing out of the minor groove (see Scheme 4b). Moreover, the enediyne bridge is no longer able to abstract H from DNA in the latter situation. The favorable docking orientation is supported by a number of individual

(74) Wilhelmsson, L. M.; Esbjörner, E. K.; Westerlund, F.; Norden, B.; Lincoln, P. *J. Phys. Chem. B* **2003**, *107*, 11784.

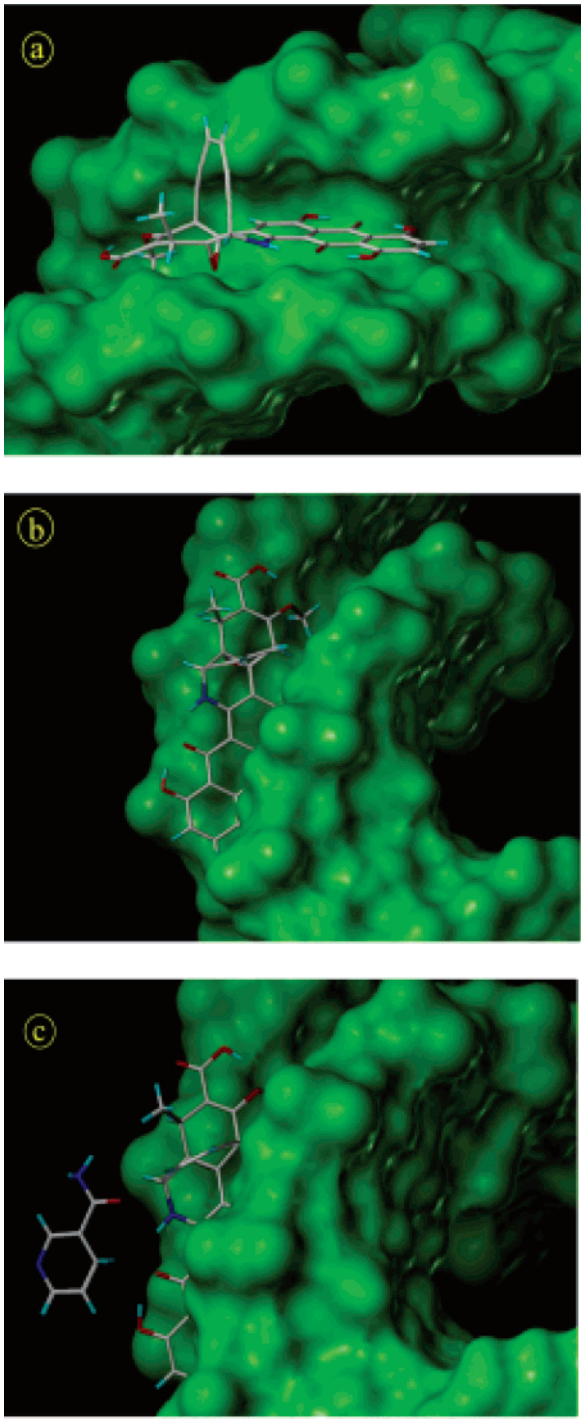

Figure 4. (a) Positioning of dynemicin A (**1**) in the minor groove of the duplex 10-mer B-DNA sequence d(CTACTACTGG)·d(CCAGTAGTAG). DNA is depicted using a Conolly surface. The atom N1H is pointing to the front. (b) Accessibility of **1** within the minor groove of DNA (Conolly surface). (c) Attack of the reducing agent NADPH (only nicotinamide part shown) at the keto group C20O6. **1** optimized with B3LYP/3-21G. DNA minimized with the Amber94 force field.

interactions: (a) the anthraquinone part can move deeper into the minor groove without being hindered by rings D and E. (b) The hydrophilic carboxylate group points out of the minor groove so that it can be stabilized by solvation in aqueous solution. In the unfavorable docking situation, the carboxylate group would come in contact with either hydrophobic groups or the negatively charged phosphate groups, which both lead

Table 5. Docking Energies ΔE_b and H Abstraction Distances of the Insertion Mechanism for the Dynemicin A Cyclization Structures[a]

structure	ΔE_b	abs site[b]	C27···H
1	−7.6	G7(H5′)	2.707
6	−7.3	G7(H5′)	2.764
TS(6−7)	−6.1	A6(H5′)	2.233
7-S	−6.5	G7(H5′)	2.694
TS(7−8)	−6.6	G7(H5′)	2.693
8	−7.0	T5(H4′)	3.011

[a] Orientation in the docking site and docking energies obtained with AutoDock, as described in Section 2 of the text. Energy differences in kcal/mol, distances in Å. [b] Abs site is the abstraction site, indicating the nucleotide and the hydrogen aligned for abstraction. C27···H denotes the distance between C27 (Scheme 1) and the closest H atom.

Scheme 4. Schematic Representation of the Global Shape of **1** in the Form of a Sickle: The Sickle Has to Face the Abstraction Site (a) Rather than Turn Away from It (b) for Carrying out H Abstraction

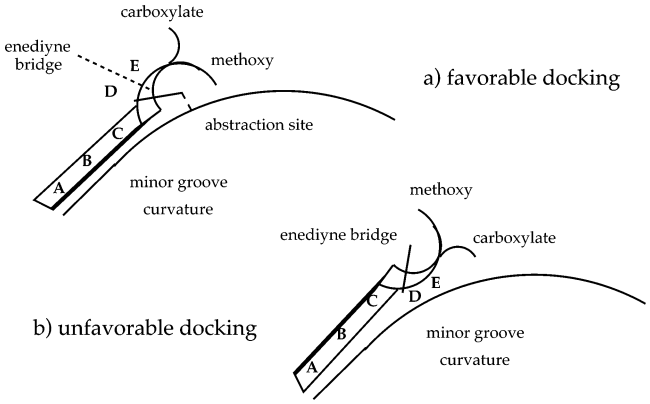

to destabilization. (c) The epoxide establishes a H-bond with a nucleotide of the lower strand (Figure 4a). If it opens and forms an alcohol, the latter acts as a H-bond donor for one of the O atoms belonging to the next phosphate group. Hence, the docking position shown in Figure 4 and schematically in Scheme 4a is clearly stabilized, relative to other docking orientations involving insertion along the minor groove. It guarantees (as indicated in Scheme 4a) the correct alignment for abstraction of a H atom from the next nucleotide.

It is interesting to see that the epoxide of **1** is hidden in the minor groove (Figure 4a) and cannot be directly attacked by an electrophile from the front or a nucleophile from the back (compare with Figures 4b and 4c, which give top views of the minor groove, indicating those parts of the enediyne protruding to the outside of the minor groove). However, one of the keto groups of the anthraquinone moiety is pointing away from the minor groove and is protected only by intramolecular H-bonding involving O5H and N1H (Scheme 1, Figure 4b). In Figure 4c, the nicotinamide part of NADPH is shown, which can attack with its CH_2 group the keto group of **1**. The transfer of two electrons into the anthraquinone π-system followed by double protonation at O6 and O3 leads to **4** (there is sufficient space in the minor groove for a water molecule to squeeze in from the side of ring A and to deliver a proton to O3; compare Figures 4a and 5).

Modeling the formation of **4** with the help of reaction 7 shown in Scheme 5 (nicotinamide is used instead of NADPH; H_3O^+ delivers a proton), we obtain at the B3LYP/6-31G(d) level of theory a reaction energy of −33 kcal/mol. The conversion of **4** into **5** (Scheme 5, reaction 8) is exothermic by 24 kcal/mol,

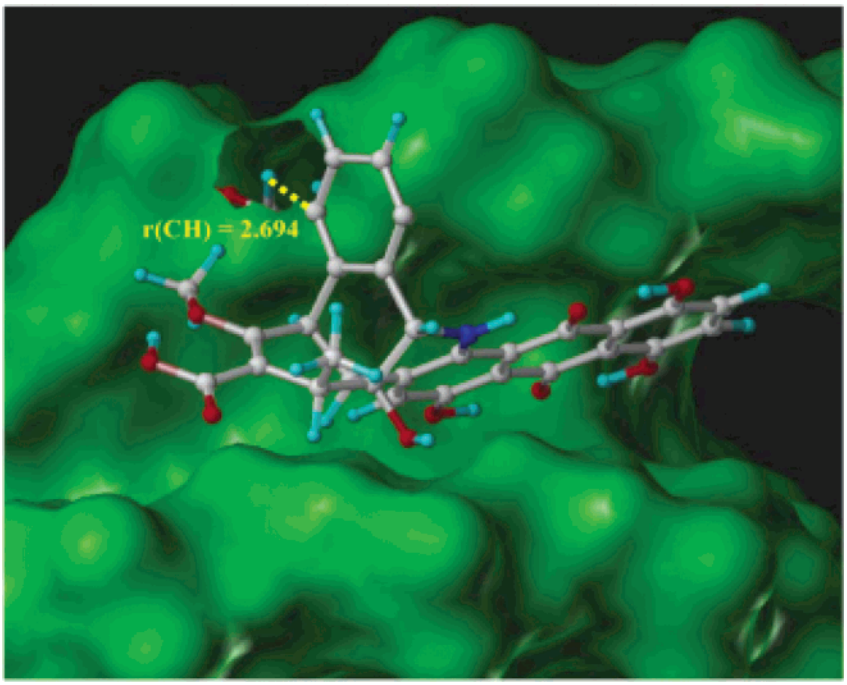

Figure 5. Abstraction of H5′ from nucleotide G7 of the DNA sequence by **7-S**. DNA is presented by a Conolly surface opened at the H-abstraction site. Distances in Å. Angles in deg.

Scheme 5. Exothermicities of the Triggering Reactions 7, 8, and 9

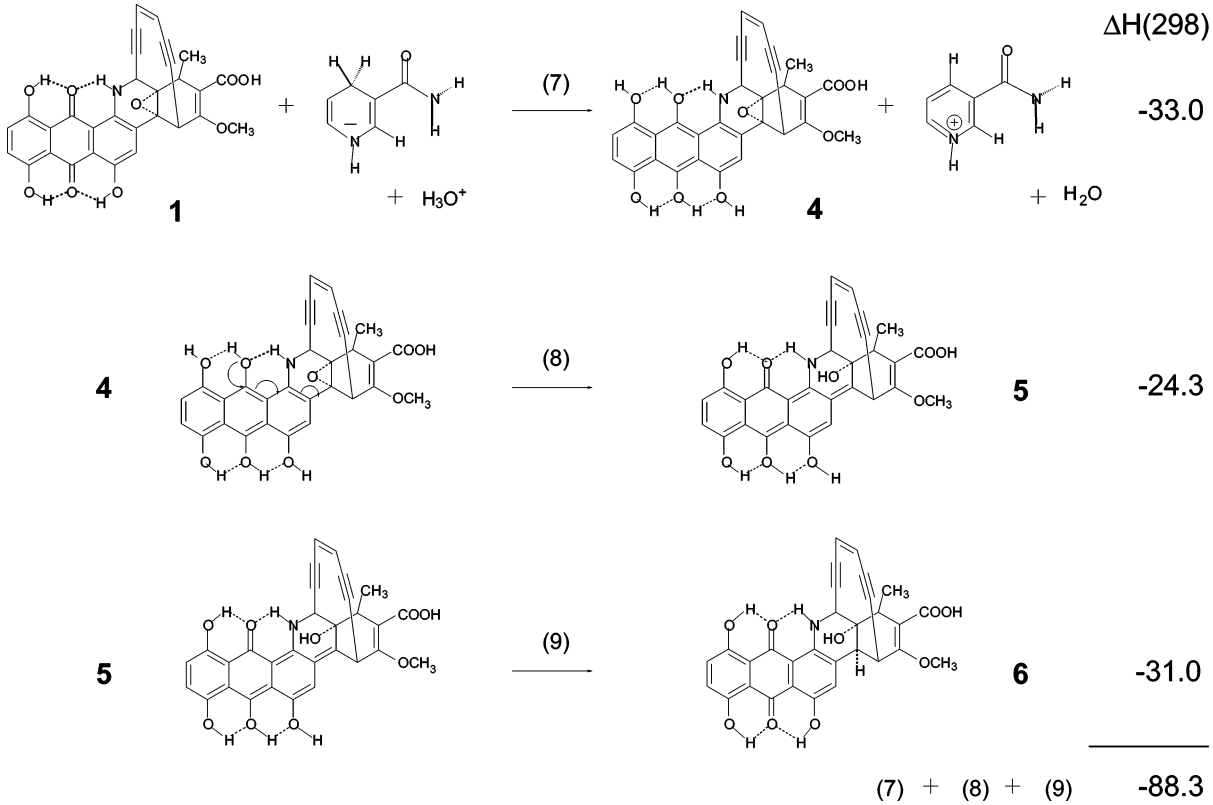

which corresponds mainly to the strain relief caused by epoxide opening. Finally, the anthraquinone moiety is reinstalled in reaction 9 leading from **5** to **6**, which again is exothermic (−31 kcal/mol, Scheme 5). The triggering process (7) + (8) + (9) is exothermic by 88 kcal/mol. Since electron transfer and protonation in reaction 7 do not require any significant activation enthalpy, the triggering process should depend on the reconfiguration of the H-bonds, which according to test calculations requires 10−15 kcal/mol. Once the reaction has started, by a collision of a reducing agent with docked **1** (see Figure 4c), the triggering process cannot be stopped, because in each step more energy is set free than is needed to surmount the reaction barrier for the following step. Energy dissipation will consume a large part of the total reaction energy, although it is likely that part of the triggering energy is directly used for the Bergman reaction.

The triggering of **1**, resulting in the formation of **6**, hardly changes the insertion energy of the enediyne ($\Delta E = -7.61$ kcal/mol (**1**), $\Delta E = -7.32$ kcal/mol (**6**), Table 4). Moreover, the overall orientation of the enediyne in the minor groove is retained. In **TS(6−7)**, the placement of the molecule in the minor groove differs from that obtained for **1** and **6** in that the structure is shifted slightly along the minor groove so that the closest abstractable hydrogen atom is now the H5′ atom of the nucleotide one base pair to the 3′ side (A6) (r(CH) = 2.233 Å for **TS(6−7)**, Table 4). This shift along the minor groove is also accompanied by a destabilization of the complex, reflected in a decrease of the binding energy by ca. 1 kcal/mol ($\Delta E = -6.12$ kcal/mol for **TS(6−7)**, Table 4). This implies that the activation enthalpy of the Bergman reaction increases for inserted **6** to 17.9 kcal/mol (Table 3), contrary to the intercalation mode (Table 4).

Upon completion of the cyclization process and the formation of the singlet biradical **7-S**, the complex becomes slightly more stable ($\Delta E = -6.54$ kcal/mol, (**7-S**), Table 4), and the alignment of the warhead with the proposed abstraction site is restored (r(CH) = 2.694 Å (**7-S**), Table 4). Furthermore, **7-S** is rotated clockwise when looking from the anthraquinone moiety to the enediyne unit (Figure 5). Through this rotation, it appears that a movement of the warhead is started that brings it slightly out of the minor groove and into the right position for H abstraction.

In Figure 5, the H atom to be abstracted is shown at a distance of 2.694 Å from the radical carbon atom. Furthermore, the angle between the bond C27C28 of the *para*-benzyne ring and the C27···H bond vector is 127.7°, which indicates a reasonable alignment of the H atom for the abstraction; that is, the H atom approaches roughly in the direction of the singly occupied orbital. However, there are two reasons why an effective H abstraction is still hindered in the situation shown in Figure 5.

(a) For an optimal abstraction, the H atom should lie in the same plane as the benzyne ring, in accordance with the C orbital containing the unpaired electron. Since the abstractable H lies 30° out of the plane of the benzyne ring in the predicted arrangement, there must be some rehybridization of the singly occupied orbital. Test calculations reveal that this is not a problem.

(b) The C−H bond to be broken must be linearly arranged with the orbital containing the single electron. In the case of H5′, the CHC angle is close to 150° and the CH bond is rotated by 105° to the side. Thus, **7-S** has to rotate sidewise out of the minor groove keeping the distance between C27 and H5′ short and aligning C27···H5′−C linearly to reduce the barrier for H abstraction to 12 kcal/mol. The phenyl radical formed in this way will immediately abstract another H atom from one of its next collision partners. This latter abstraction is likely to occur outside the minor groove and involve a solvent molecule.

We conclude that inserted rather than intercalated **1** will lead via **6** to single-stranded scissions. This will most likely result in an increased flexibility of the DNA in the region of the H abstraction, and this flexibility may result in the much easier alignment of a second enediyne **1** and another single-stranded scission of the second strand close to where the first strand was damaged. Certainly, the double-stranded scission cannot occur in a simultaneous abstraction step, as the second radical center is directed out of the minor groove (Figure 5). This finding is in line with previous experimental[11,16] proposals for a two-step abstraction process for **1**, despite the difference in the proposed binding mechanism (i.e., insertion vs intercalation). We note that in the intercalation mode a double-stranded scission should be possible if H abstraction were possible at all. We consider the observed two-step abstraction mechanism another argument for the insertion−intercalation model suggested in this work.

The alternative to the abstraction of H atoms by **7-S** would be the reopening of the warhead to the acyclic enediyne system (**8**) via **TS(7−8)**. If **8** would be formed (which can actually be excluded in view of the high rearrangement barrier; see Tables 2 and 3), this would lead to a large shift of **8** in the minor groove, in order for its extended warhead to protrude from the DNA structure. Clearly **8** has strongly different docking properties that are not in line with those of **1**.

6. Conclusions

We have applied in this work a variety of different methods stretching from quantum mechanics to molecular mechanics (DFT, BD(T), ONIOM, CHARMM, Amber, molecular modeling, docking, puckering analysis) to describe the biological activity of the 2*S*,7*R*-enantiomer of dynemicin A (**1**). We could confirm that **1** is a typical intercalator and were able to explain trends in measured intercalation energies for several derivatives of **1**. However, we also have shown that the intercalation model alone cannot explain triggering and the biological activity of dynemicins. Therefore, we propose in this work an insertion−intercalation model, which is based on an equilibrium between insertion and intercalation modes. The insertion−intercalation model can explain the following observations.

(a) Triggering takes place in the insertion rather than the intercalation mode. According to calculated and measured binding energies (insertion, estimated: −5 kcal/mol; intercalation, measured: −6.5 kcal/mol),[14] there should always be a small amount (ca. 7%) of **1** in the insertion mode.

(b) Once triggered, enediyne **6** has sufficient energy either to undergo the Bergman reaction while inserted in the minor groove or to intercalate. Both processes possess comparable activation energies so that one can expect half of the molecules to form biradical **7-S** in the insertion mode and half of them in the intercalation mode. However, only the former can abstract a H atom from the backbone.

(c) The insertion−intercalation model explains also why strong intercalators (dynemicin derivatives with a methylester rather than a COO^- group that have an intercalation free energy of −9 kcal/mol or larger in magnitude[14]) suppress any biological activity of dynemicin: The insertion−intercalation equilibrium is shifted totally to the intercalculation side. There are no molecules in the insertion mode. Since triggering is a rare event, there are just a few dynemicin molecules that could be triggered before intercalation.

(d) In the insertion mode, **1** is perfectly positioned for the triggering reaction, whereas freely floating in the cell a reactive collision between **1** and $NADPH^+$ is less likely.

Important conclusions can also be drawn from our calculations concerning the triggering reaction and the interactions of **1** or **6** with DNA.

(1) The Bergman reaction of untriggered **1** is effectively blocked by a strain device: The epoxide ring forces rings D and E in boat or half-boat forms that squeeze the enediyne unit

in ring F apart and, as such, raise the barrier to cyclization up to 52 kcal/mol.

(2) The triggering of **1**, by reducing agents such as NADPH, was calculated to be exothermic by 88 kcal/mol. There can be three steps (Scheme 5), each of which is exothermic (−33, −24, −31 kcal/mol). Part of this energy gain can initiate the Bergman reaction. The triggering reaction is not hindered when **1** is inserted in the minor groove. There is sufficient space for an attack of NADPH at the nicotinamide side, followed by electron transfer and protonation.

(3) The calculated activation enthalpy of triggered dynemicin A, **6**, is 16.7 kcal/mol and fits by this into a enthalpy window from 11 to 23 kcal/mol that guarantees biological activity. Triggering has two effects on the Bergman activation enthalpy. It relieves 57 kcal/mol of strain energy in **TS(6−7)** of the Bergman reaction, but just 22 kcal/mol (rather than 33 kcal/mol) for **6**. The remaining 11 kcal/mol are stored in the enediyne ring, F, thus destabilizing the reactant and decreasing, in this way, the activation enthalpy so that it drops into the window determining biological activity.

(4) The singlet biradical **7-S** is kinetically stable and can abstract H if appropriately positioned in the minor groove. The activation enthalpies for the retro-Bergman reactions are 19.5 and 21.8 kcal/mol. The singlet−triplet splitting of **7** is 3.5 kcal/mol and indicates that **7** has a similar reactivity as *p*-benzyne (Table 3).

(5) During the Bergman reaction of **6**, there are changes in the insertion orientation starting with **TS(6−7)** and being obvious for **7-S** (see Figure 5). The positional change increases the activation enthalpy of **6** from 16.7 to 17.9 kcal/mol in the minor groove.

(6) In order for atom G7-H5′ to be abstracted, **7-S** has to continue the movement started with the Bergman reaction: It has to rotate out of the minor groove to abstract atom G7-H5′. The phenyl radical generated will abstract a second H atom from another source (e.g., a solvent molecule). This confirms that **6** can initiate only a single-strand scission in the insertion mode and that a second molecule is needed to complete the double-strand scission. This explains the high ratio of single- to double-strand scissions observed for **1**.

(7) If **7-S** succeeds in opening to the dynemicin isomer, **8**, docking is no longer possible and **8** is released from the minor groove.

The insight provided in this work reveals the importance of stereochemical and environmental effects for the observed biological activity of **1**. The role of the triggering device and delivery system is emphasized and has led to the proposal of a new docking mechanism for this molecule. We note that studies concentrating just on the warhead outside the minor groove are not capable of unraveling the biological activity of **1**, as for this purpose the proposed mechanism needs to rationalize all experimental observations. The new insights gained in this work will be used to design on the basis of **1** a more powerful, nontoxic antitumor lead.[74]

Acknowledgment. T.T. thanks M. Waller for construction and minimization of the primary DNA sequence. E.K. and D.C. thank the National Supercomputer Center (NSC) at Linköping for a generous allotment of computer time.

Supporting Information Available: Details on the puckering analysis of rings D and E (5 pages, print/PDF), the calculation of the strain energies given in Scheme 3, the influence of the partial charges on the binding energies, and energies and Cartesian coordinates of the dynemicin structures investigated in this work (16 pages, print/PDF). This material is available free of charge via the Internet at http://pubs.acs.org.

JA046251F

(75) Kraka, E.; Cremer, D.; Tuttle, T. To be published.